applied sciences

MDPI

Article

Environmental Changes and Cultural Transitions in SW Iberia during the Early-Mid Holocene

Cristina Val-Peón [1,*], Juan I. Santisteban [2], José A. López-Sáez [3], Gerd-Christian Weniger [4] and Klaus Reicherter [1]

1 Institute of Neotectonics and Natural Hazards, RWTH Aachen University, 52062 Aachen, Germany; k.reicherter@nug.rwth-aachen.de
2 Department of Geodynamics, Stratigraphy and Paleontology, Fac. Geological Sciences, Complutense University of Madrid, 28040 Madrid, Spain; j.i.santisteban@geo.ucm.es
3 Environmental Archaeology Research Group, Institute of History (CCHS), C.S.I.C., 28037 Madrid, Spain; joseantonio.lopez@cchs.csic.es
4 Institute for Prehistoric Archaeology, Cologne University, 50923 Köln, Germany; weniger@neanderthal.de
* Correspondence: c.val-peon@nug.rwth-aachen.de

Abstract: The SW coast of the Iberian Peninsula experiences a lack of palaeoenvironmental and archaeological data. With the aim to fill this gap, we contribute with a new palynological and geochemical dataset obtained from a sediment core drilled in the continental shelf of the Algarve coast. Archaeological data have been correlated with our multi-proxy dataset to understand how human groups adapted to environmental changes during the Early-Mid Holocene, with special focus on the Mesolithic to Neolithic transition. Vegetation trends indicate warm conditions at the onset of the Holocene followed by increased moisture and forest development *ca*. 10–7 ka BP, after which woodlands are progressively replaced by heaths. Peaks of aridity were identified at 8.2 and 7. 5 ka BP. Compositional, textural, redox state, and weathering of source area geochemical proxies indicates abrupt palaeoceanographic modifications and gradual terrestrial changes at 8.2 ka BP, while the 7.5 ka BP event mirrors a decrease in land moisture availability. Mesolithic sites are mainly composed of seasonal camps with direct access to the coast for the exploitation of local resources. This pattern extends into the Early Neolithic, when these sites coexist with seasonal and permanent occupations located in inland areas near rivers. Changes in settlement patterns and dietary habits may be influenced by changes in coastal environments caused by the sea-level rise and the impact of the 8.2 and 7.5 ka BP climate events.

Keywords: palaeoenvironment; mesolithic; neolithic; palynology; geochemistry; SW Iberian Coast

Citation: Val-Peón, C.; Santisteban, J.I.; López-Sáez, J.A.; Weniger, G.-C.; Reicherter, K. Environmental Changes and Cultural Transitions in SW Iberia during the Early-Mid Holocene. *Appl. Sci.* **2021**, *11*, 3580. https://doi.org/10.3390/app11083580

Academic Editor: Jordi Revelles

Received: 29 March 2021
Accepted: 13 April 2021
Published: 16 April 2021

1. Introduction

The Early-Mid Holocene period is characterized by several environmental changes, such as the postglacial marine transgression, an increase of temperatures, and the existence of diverse episodes of ice-rafted debris in the North Atlantic Ocean. Littoral areas suffered a rapid transformation resulting from the inundation of the fluvial valleys and the progressive development of diverse coastal features. From a different perspective, the vegetation adapted to the new climatic-edaphic conditions and reacted to abrupt episodes, the so called Bond events, which are associated to dry conditions in the Mediterranean region [1]. However, the Early-Mid Holocene was not only defined by unique environmental changes, but by important cultural transformations within hunter-gatherer groups and the adoption of new subsistence strategies.

The process of neolithization in Southwestern Iberia is controversially disputed and different theories attempt to explain its origin. Some authors interpret it as a maritime pioneer colonisation of depopulated regions by Neolithic groups from the Western Mediterranean [2], while others propose indigenous origins defined by the continuity of local

Mesolithic groups in certain regions [3], suggesting that the beginnings of agriculture could have had an autochthonous nature [4]. Many authors consider that the area of Andalusia, the Algarve, and the Moroccan Atlantic fringe have shared similar traits during this process [5], which would explain the existence of Neolithic "enclaves" with specific regional features [6] or a southern neolithization route along the North African coast [7,8]. The inherently intricate interpretation of such a complex process is, in this case, weighed down by the lack of absolute datings in clear stratigraphic sequences, and the absence of information regarding the Mesolithic period at a regional scale [9].

Recent palaeogenetic studies have shed light on this complicated situation, confirming that Southern Iberian Neolithic humans share the same genetic composition as the Cardial Mediterranean culture that reached Iberia *ca.* 7.5 ka BP [10]. These early Neolithic Iberian groups present genetic differences with the early Neolithic central European farmers, pointing toward two different migrations and linking all Neolithic Iberians with the first migrants that arrived with the initial Mediterranean Neolithic wave of expansion [11]. It is evident that these Iberians mixed with local hunter-gatherers, maintaining and thus expanding their subsistence strategies. However, it is assumed that this process was not homogeneous and the introduction of new elements, such as food production techniques, can hardly be dissociated from the heterogenous geography, the environmental diversity, and the influence of local groups. Therefore, further research is needed to explain differences in both Mesolithic and Neolithic cultures at the regional scale, as well as to complete the complex environmental puzzle of this area.

Studies integrating archaeological and palaeoenvironmental data from a long-term perspective can provide a critical framework to examine the resilience of human groups to past and current global changes. Thus, this work focuses on the palaeoenvironmental reconstruction of the southwestern Iberian littoral area, with special focus on the occidental Algarve coast, in the course of the Mesolithic and Neolithic periods. We contribute with a new environmental dataset of palynological and geochemical data to discuss and define changes in the vegetation, reconstructing coastal landscapes, and understanding how human groups adapted to these transformations.

1.1. Archaeological Context

Two main clusters of Mesolithic and Neolithic sites are located in the southwestern Iberian coast, one in the westernmost extreme of the Algarve littoral, and the other one in the southeastern region of the Gulf of Cádiz towards the Strait of Gibraltar (Figure 1; Supplementary data).

Most of all the Mesolithic sites are found in the Cape São Vicente region. They constitute shell-middens of different sizes (Castelejo, Barranco das Quebradas, Rocha das Gaivotas) and open air sites (Armação Nova, Vale Boi) interpreted as seasonal occupations based on the exploitation of coastal and/or lithic resources [12,13]. Near the Straits of Gibraltar, the only site for this period is considered as a single occupation based on the exploitation of marine resources and hunting (Palmones), although there is some controversy about its chronology [14,15]. The majority of these sites is located close to marine environments or in transitional areas between fluvial and marine influences.

Several Neolithic sites have been discovered in both areas. In the Cape São Vicente region, shell-middens (Alcalar 7, Ribeira de Alcantarilha) and temporary open-air sites (Vale Santo I, Padrão) based on the seasonal exploitation of marine and lithic resources are still present [12]. Moreover, some Mesolithic sites revealed later Neolithic layers (Castelejo, Barranco das Quebradas, Rocha das Gaivotas, Vale Boi) [12,13,16]. Two necropolis caves (Ibn-Ahmmar, Algarão da Goldra) were also assigned to this period. There is one site considered a residential basecamp (Cabranosa), a settlement suggesting an obvious sedentary occupation with hut structures and grave burials (Castelo Belinho), and a possible long-term settlement in a beach environment (Praia do Forte Novo) which is considered a salt production site by some authors [17]. Many of these new Neolithic sites are located in fluvial environments some

kilometres inland, if compared with those belonging to the Mesolithic (Alcalar 7, Ribeira de Alcantarilha, Castelo Belinho, Ibne-Ahmmar, Algarão da Goldra).

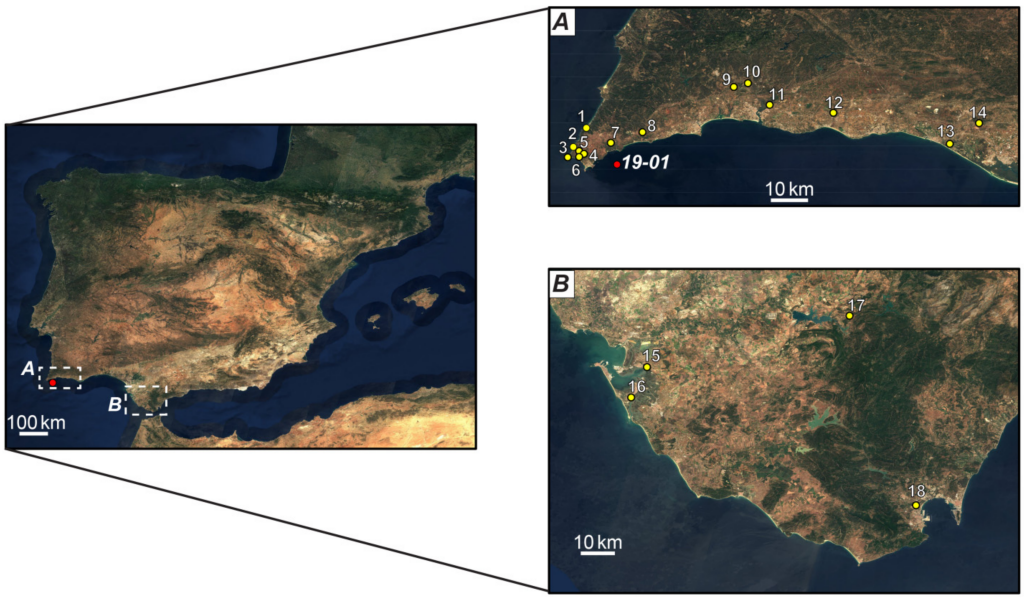

1	Castelejo	**7**	Padrão	**13**	Praia do Forte Novo
2	Barranco das Quebradas	**8**	Vale Boi	**14**	Algarão da Goldra
3	Rocha das Gaivotas	**9**	Alcalar 7	**15**	El Retamar
4	Armação Nova	**10**	Castelo Belinho	**16**	Campo de Hockey
5	Vale Santo I	**11**	Ibne-Ahmmar	**17**	La Dehesilla
6	Cabranosa	**12**	Ribeira de Alcantarilha	**18**	Palmones

Figure 1. Map of the Iberian Peninsula indicating: the sediment core 19-01 (red dot), the distribution of archaeological sites in the region of the Algarve (**A**), and in the Southeast of the Gulf of Cádiz (**B**).

In the southeastern area of the Gulf of Cádiz it is possible to identify varying typologies of archaeological sites with Neolithic occupations: a single human occupation (El Retamar) based on the exploitation of marine resources, hunting, and animal domestication [18,19], a permanent settlement (Campo de Hockey) with a large necropolis [20–22], and a necropolis cave (La Dehesilla) [23]. With the exception of the cave situated in a mountainous area, all other sites are located in the marine-fluvial environments of the Cádiz Bay.

1.2. Regional Settings

The study area comprises the southwestern coastal region of the Iberian Peninsula framed by the Atlantic Ocean and located north of the Africa-Iberia plate boundary. The westernmost part is a Meso-Cenozoic sedimentary basin overlying Carboniferous basement, which extends offshore as far as 100 km south [24]. However, most of the coast is dominated by Neogene basins defined by the presence of several estuaries conforming littoral lowlands. Some of them are sheltered by spits, with marshlands extending several kilometers inland [25,26]. These characteristics are mainly due to the morphology of the coast and the prevailing winds from SW that generate a littoral drift towards the East and SE of the Gulf of Cádiz, being responsible for the formation of beach and barrier systems that partially close some estuaries [25,27].

The SW Iberian Peninsula has a Mediterranean climate with oceanic influence that can be defined by two climatic zones described by Köppen-Geiger [28]: a temperate climate with hot summers in oriental and inland areas (Csa), and a temperate climate with warm summers in occidental areas and the littoral (Csb). Considering both zones, the annual

average minimum temperature oscillates between 12.5 °C and 15 °C, and the annual average maximum temperature ranges from 22.5 °C to 25 °C [29]. The average total annual precipitation fluctuates between 500 mm and 1000 mm, mostly concentrated during winter season [29] The thermomediterranean belt of the coastal lowlands is defined by different ecosystems and vegetal ecological associations. Woodlands are mainly composed of evergreen (*Quercus suber*, *Q. rotundifolia*) and deciduous oaks (*Q. faginea*, *Q. estremadurensis*), together with some Mediterranean species, such as Olea europaeae subs. sylvestris or Juniperus oxycedrus, among others. Pre-forest scrubs are dominated by Quercus coccifera, Phillyrea angustifolia, Pistacia lentiscus, Rhamnus sp., and Juniperus sp, while riparian communities are formed by *Alnus glutinosa*, *Salix* sp., Fraxinus angustifolia, and Tamarix sp. [30–33]. Heathlands are well represented by different genera of Ericaceae that grow on acidic low fertility soils, under high humidity levels and strong oceanic conditions [34]. In littoral areas and interdunal valleys the vegetation is mainly composed of Pinus pinaster, *P. pinea* and *P. halepensis*. The most representative herbaceous vegetation of the stable dunes are: *Polygonum maritimum*, *Artemisia crithmifolia*, *Eryngium maritimum*, *Cyperus capitatus*, *Anthemis maritima*, *Silene* sp., *Juniperus* sp. [35]. Freshwater marshlands include species of Cyperaceae and *Isoetes* spp., *Typha* sp., Hypericum tomentosum, and Phragmites australis, while saltmarshes are dominated by species of Chenopodiaceae and some taxa such as Apium graveolens, Aster tripolium, Limonium, Juncus maritimus, and others [30,36,37].

2. Materials and Methods

Twin sediment cores 19-01 and 19-02 (referenced as GeoB23519-01/-02 in the MARUM core repository in Bremen, Germany) were retrieved in the Algarve continental shelf (37° 00.656, 008° 52.247 and 37° 00.654, 008° 52.26, respectively) at *ca.* 65 m water depth and approximately 3 km from the coast using a vibracorer. The 3.64 m-long core 19-01 was sampled for palynological analysis and the neighboring core 19-02 (3.62 m-length) is added to increase data and resolution on sedimentation rates and chronology. In both cores, stratigraphic units were identified by visual description of the sediment.

From bottom to top (Figure 2), both cores are composed of greenish fine sands covered by muddy sediments and capped by coarse silt to silty sand (uppermost 1.5 m). Shells are common as well-preserved specimens and the clastic fraction is composed by bioclasts, siliciclastics, and lithic fragments.

X-ray fluorescence scans (XRF) were measured using an ITRAX core scanner (resolution 2 mm, 20 s exposure time, 30 kV, 55 mA). Carbonate (Ca, Sr), siliciclastic (Si, Al, Ti, Zr, Rb), organic matter (Br, Mo incoherent and coherent scatter [Mo inc, Mo coh]), and redox geochemical (Mn, Fe) proxies were chosen (Figure 2) and some useful ratios were analyzed (Ca/Si, Si/Al, Zr/Al, Zr/Rb, Mn/Fe, Mo inc/coh) [38]. Anomalous values were removed by comparison to the core photographs to minimize the effect of coarse grains, cracks, and surface irregularities. The remaining data were normalized by count per row to unit by column and smoothed with an arbitrary 11-point running mean filter to reduce the inherent data noise.

Seven articulated bivalves from core 19-01 and six more articulated valves from 19-02 were ^{14}C-dated at the Beta Analytic Inc. and the University of California-Irvine (USA). Calibration was performed with CALIB 8.2 [39] using the Marine20 calibration dataset [40] and different ΔR calculated from the original datasets of [41–45] by using the online application of [46] (Table 1). After comparison of the sedimentological and geochemical logs, it was possible to correlate both cores by depth. The age model is based on a simple linear interpolation and sedimentation rates were calculated for each dated interval (Figure 3).

Palynological samples were collected from core 19-01 with an interval of 3–7 cm. All samples were chemically treated with HCl to remove carbonates, KOH to remove humic acids, and sodium polytungstate (SPT: $3Na_2WO_4 \cdot 9WO_3 \cdot H_2O$) at 2.0–2.1 cm^3 for densimetric separation. The final residue obtained after the treatment was mounted on slides with the use of glycerol mixed with phenol. Palynomorphs were counted using an optical microscope at 400× and 1000× to a minimum pollen sum of 150 terrestrial pollen grains.

Fossil pollen grains, spores, and non-pollen palynomorphs were identified using published keys [47–52] and the modern pollen reference collection of the CSIC in Madrid (Spain). Microcharcoal particles >125 µm were counted alongside the identification of pollen grains and interpreted as indicators of regional fires [53]. Pollen and microcharcoal concentrations (grains/gr and particles/gr of dry sediment, respectively) were estimated by adding one Lycopodium clavatum tablet to each sample [54]. Diagrams were plotted versus age using TiliaIT software (version 2.1.1, Illinois State Museum, Research and Collection Center. Springfield, IL, USA) Palynological assemblage zones were determined by Constrained Cluster Analysis Sum Squares (CONISS) based on a square root transformation (Edwards & Cavalli-Sforza chord distance).

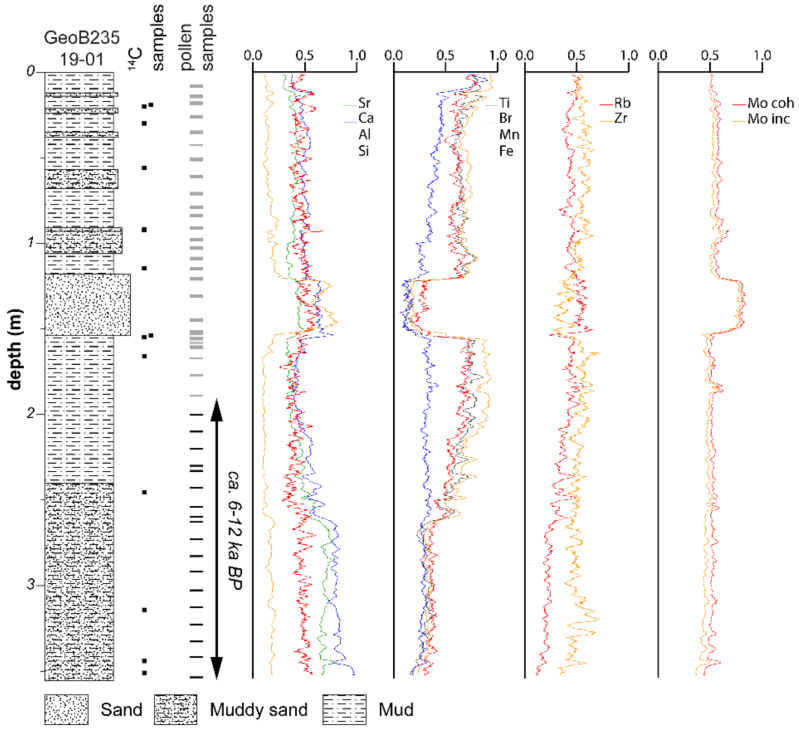

Figure 2. Lithological log, location of 14C and pollen samples (black: samples used in this study) and selected XRF parameters for core 19-01.

Table 1. Radiocarbon samples and calibration parameters and results. * and italics: rejected sample due to possible reworking.

Core	Lab. Code	Depth (m)	^{14}C Age (yr BP)	Error	ΔR	Error	Age Cal. BP Median	2σ Range (cal. BP)
GeoB235 19-01	236164	0.21	650	15	−49	121	177	0–399
	Beta-526115	0.57	2610	30	−73	140	2212	1829–2622
	236165	0.93	3205	15	−36	152	2903	2505–3312
	236166	1.55	4245	15	50	152	4090	3660–4515
	236167	1.67	5390	20	407	165	5098	4673–5523
	236168	3.16	9230	20	740	225	8892	8354–9445
	236169	4.46	9530	20	−46	206	10,292	9658–10,910
GeoB235 19-02	Beta-512669	0.20	600	30	−49	121	148	0–367
	Beta-512670	0.31	1570	30	−194	125	1155	864–1453
	Beta-512668 *	*1.16*	*4280*	*30*	*50*	*152*	*4136*	*3693–4564* *
	Beta-512667	1.56	4330	30	50	152	4201	3759–4641
	Beta-512666	2.47	7910	30	301	201	7893	7488–8328
	Beta-512665	3.53	10,360	30	−46	206	11,458	10,797–12,104

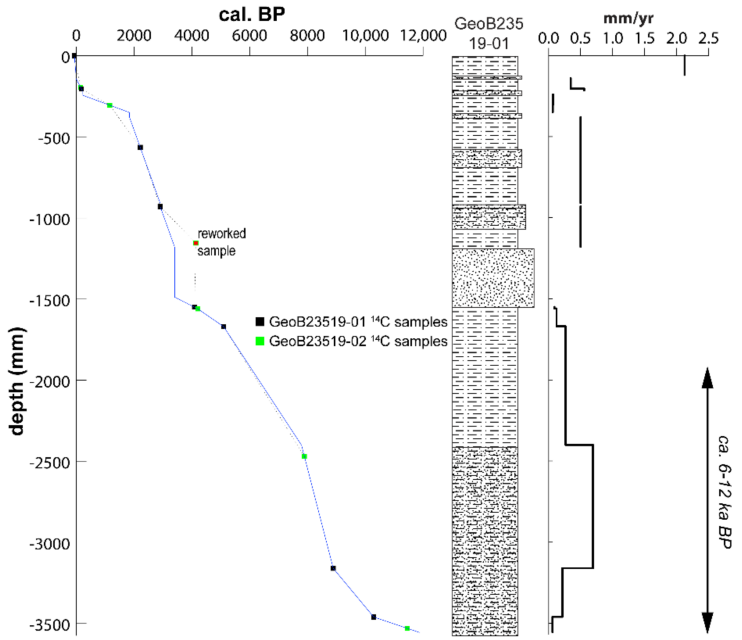

Figure 3. Age model, sedimentation rates and lithological log for core 19-01. Key for lithologies as Figure 2.

In the synthetic diagram main categories are organized in the following way: High-mountain pines (*Pinus sylvestris-nigra* type), Mediterranean pines (*Pinus halepensis-pinea* type and *Pinus pinaster*), Mediterranean woodland (evergreen *Quercus*, *Olea europaea*), Mediterranean shrubland (*Phillyrea, Arbutus*), Riparian woodland (*Alnus, Fraxinus, Salix*), Mesophilous trees (deciduous *Quercus, Acer, Corylus, Betula*), Heathlands (*Erica* type, *Calluna*), Xerophytic taxa (*Juniperus, Ephedra fragilis* type, *Artemisia*), Asteraceae (Carduoideae, Asteroideae, Cichorioideae), Ferns & Mosses (see Figure 7), Hygro-hydrophytic herbs (*Typha,* Cyperaceae, *Callitriche, Potamogeton*), Coprophilous (*Coniochaeta* /HdV-172, *Sporomiella*/HdV-113, *Sordariaceae, Chaetomium*), and Erosive processes (*Glomus* sp., *Pseudoschizaeae circula*).

Pollen percentages for terrestrial taxa were calculated against the main sum of terrestrial grains, while percentages for aquatics, spores, and *Pinus* were calculated against the total sum of all pollen and spores. Pinus grains were excluded from the main sum because they are considered to be over-represented in marine sediment cores because of its extensive dispersal ability and buoyancy (Hopkins, 1950). However, morphometric analysis of their pollen grains was done using a measurement of the grain diameter, excluding sacci [55–57].

3. Results

3.1. Age-Depth Model

According to the proposed age model, the period between 12 ka and 6 ka BP is placed in the lowermost 1.5 m of the core. From *ca.* 12 ka BP until *ca.* 8 ka BP, the sedimentation rate increases from 0.06 mm/yr to 0.69 mm/yr which corresponds to the maximum value for the Holocene in this core. From *ca.* 8 ka BP to 6 ka BP the depositional rate decreases to 0.27 mm/yr (Figure 4a).

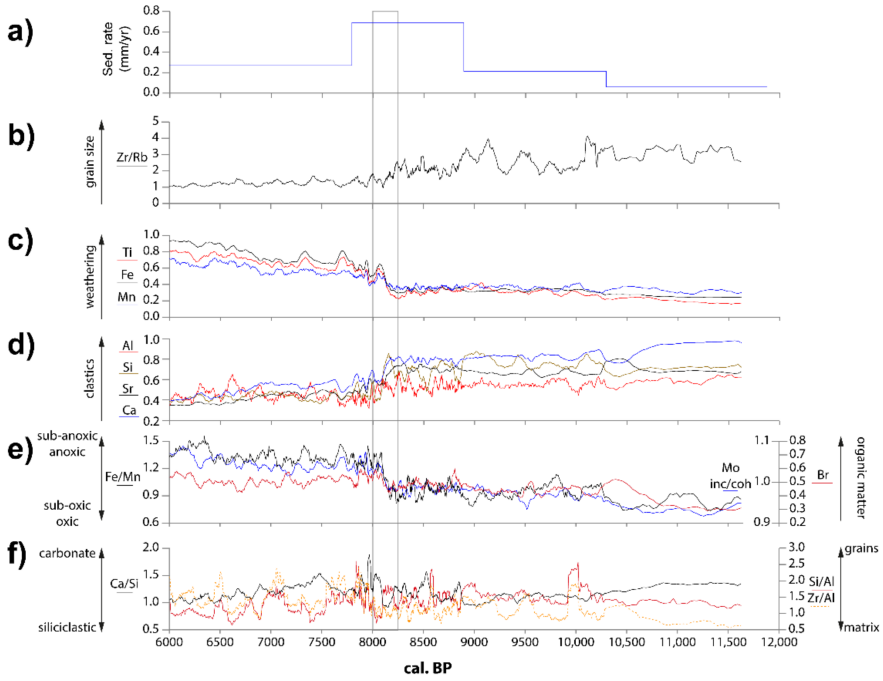

Figure 4. Age plot for the 12–6 ka BP period of the (**a**) sedimentation rate and (**b**–**f**) selected geochemical elements and ratios.

3.2. Geochemistry

The selected elements can be grouped by similar behavior along time allowing the identification of some common periods and events despite the considered parameter.

Zr/Rb ratio has been linked to grain size changes [58] and sediments older than *ca.* 8.1 ka BP show larger values and a clearer decreasing trendthan younger sediments (Figure 4b).

Ti, Fe, and Mn run almost parallel during the studied period and they can be linked to weathering of siliciclastic rocks [59]. These elements show reverse trends and peaks as compared to Zr/Rb (Figure 4c), showing large ratios and enhanced increase for the 8.2–6 ka BP period than for the Early Holocene.

Al, Si, Ca, and Sr can be correlated in the long term (Figure 4d), while they show some differences for the shorter cycles. Al and Si are interpreted as representative of terrestrial input [38]. Comparable Ca and Sr trends represent carbonates [38], and reflect high bioclastic content. All elements are components of the dominant clastic fraction, while siliciclastics depend on the terrestrial supply, carbonate variability can be due to changes on marine productivity (in situ biogenic carbonate) and this could be responsible for the out-of-phase signal for the shorter cycles. All of them show higher values for the 8–12 ka BP period, with larger amplitudes for Si, Ca, and Sr compared to the 6–8 ka BP period, when Al shows wider amplitudes reflecting the clay-richer composition of the sediments (Figure 2).

It is worth to mention the long- and short-term correlation of Br, Mo inc/coh, and Fe/Mn (Figure 4e). Br and the Mo inc/coh ratio have been used as a proxy of organic matter in marine sediments [60–62]. The Fe *vs* Mn ratios can indicate changes in the redox state [63,64], with Mn-displaced values indicating oxic conditions. All these values show a steady increase, broken by a sudden rise from 8.3 to 8 ka BP. However, they are lower for Br, mirroring the changes in clastic fraction (Al, Si, Ca, Sr).

Ca/Si ratio points to the carbonated vs. siliciclastic sources [65,66], while Si/Al and Zr/Al are used as textural proxies like sorting or grain size [38,67] (Figure 4f). These ratios show no clear trends, as those mentioned before, but they can be divided in three stages: from 12 until 8.8 ka BP, their record show low amplitude cycles that shorten their period in time, Ca/Si decreases while Zr/Al and Si/Al remain, showing a slowly increasing trend; from that time until *ca.* 7.8 ka BP, the amplitude increases while their period shortens, both Ca/Si and Si/Al increase but Zr/Al shows its average lowest values; from *ca.* 7.8 ka BP to

6 ka BP, the period of the cycles grows, while their amplitude slightly decreases without reaching values of the previous core section. Ca/Si and Al/Si values show a falling trend while Zr/Al remains nearly stable.

According to these observations, the 12–6 ka BP lapse can be split in three periods (Figure 4):

- 12–8.4 ka BP. Low values in Ti, Mn, Fe reflect reduced weathering conditions and Fe/Mn, Br, and Mo inc/coh ratios imply low preservation potential of organic matter and point to oxic conditions. Si, Al, Ca, and Sr values are high and indicate dominance of clastic/tractive deposits; the Zr/Rb values correspond to coarser grain size. Si/Al, Zr/Al, and Ca/Si values show low amplitude and slow changes, implying an environment characterized by homogeneous conditions and only disturbed by some higher energy episodes—as evidenced by increases in Zr/Rb, Zr/Al, and Si/Al. The sedimentation rate increases to its highest values.
- 8.4–8 ka BP. Amplitude and frequency of changes started to increase shortly before it. The sedimentation rate was the highest. There are marked and sudden changes for a decrease in clastic input and an increase in organic components, while the decrease in grain size and increase in weathering proxies is fast but gradual.
- 8–6 ka BP. The sedimentation rate decreases from 0.69 to 0.27 mm/yr. Clastics and grain size fall to their minimum average values but amplitude of changes increases for sorting (grains vs. matrix) proxies. Organic matter preservation increases, coincidental to sub-oxic to anoxic conditions, as well as the weathering of source areas.

3.3. Palynology

Four palynological zones were identified in this section of the GeoB235-19-01 core (Figure 5; Table 2). Oakwoods dominate the landscape between *ca.* 10–7 ka BP (Z-1, Z-2, and Z-3), after which *Erica* type progressively increases (Z-4). Cichorioideae displays constant but irregular values (Z-1 and Z-4), and the presence of pinewoods, although scarce, is constant through time with a more noticeable presence *ca.* 11.7–10 ka BP (Z-1) and *ca.* 7.6–6.5 ka BP (transition Z3–Z4).

Table 2. Pollen zone description for marine core 19-01.

Zone	Depth Range (cm)	Age Range (cal yr BP)	Pollen Signature
Z-1	354-323	11707-9242	Dominance of oakwoods (evergreen and deciduous *Quercus*: 17–20% and ~10–16% respectively) together with Cichorioideae (17–34%). *Olea* (~0–5%), *Phillyrea* (~4%), and Chenopodiaceae (~5–8%) slightly increase towards the end of the zone. *Juniperus* (~4–9%) Asteroideae (5–11%), and Poaceae (~5–9%) display discontinuous values. Pinewoods represent ~15% (*Pinus sylvestris-nigra* type, *Pinus halepensis-pinea* type, *Pinus pinaster:* ~5% each). Low % of *Isoetes* (~4–7%), and peaks of foraminiferal linings (~9–19%).
Z-2	323-263	9242-8132	Increase of deciduous and evergreen *Quercus* (~15–20% and ~17–29%), together with *Olea* (3–6%), *Phillyrea* (3–10%), and *Juniperus* (~7–11%). Slight decrease of Chenopodiaceae (3–10%) towards the end of the zone. Reduction of Poaceae (~1–5%), Asteroideae (~4–7%), and Cichorioideae (7–24%), the latter with notable peaks. Slight decrease of pinewoods (below 5% each). Progressive increase of *Isoetes* (~4–13%) and important increment of foraminiferal linings (~21–33%).
Z-3	263-230	8132-7441	Dominance of oakwoods, with peaks (deciduous: ~16–22%; evergeen: ~17–26%). Visible increase of *Erica* type (~1–11%). Decrease of *Olea* (below 3%), *Phillyrea* (~1–8%), Chenopodiaceae (~4–8%), and Cichorioideae (~7–13%). *Juniperus* (~6-12%), Asteroideae (~4–6%), and Poaceae (~2–6%) display similar values. Slight increase of pinewoods (*Pinus sylvestris nigra* type ~2–6%; *Pinus halepensis-pinea* type ~2–9%; *Pinus pinaster* ~1–5%). Increase of *Isoetes* (~12–19%) and decrease of foraminiferal linings (~7–15%).
Z-4	230-189	7441-5928	Drop of both deciduous and evergreen *Quercus* (~7–16% and ~5–12%) towards the end of the zone. Decrease of *Olea* and *Phillyrea* (both below 5%), *Juniperus* (~6–10%), and Chenopodiaceae (~3–7%). Slight increase of Poaceae (~3–8%) and Asteroideae (~5–8%). *Erica* type (~7–10%) increases approaching the end of the zone. Rise of Cichorioideae (~17–33%). Decrease of *P. sylvestris-nigra* type and *Pinus pinaster* (both below 5%) and same values for *Pinus halepensis-pinea* type (~2–9%). Increase of *Isoetes* (~14–27%) and decrease of foraminiferal linings (~2–14%).

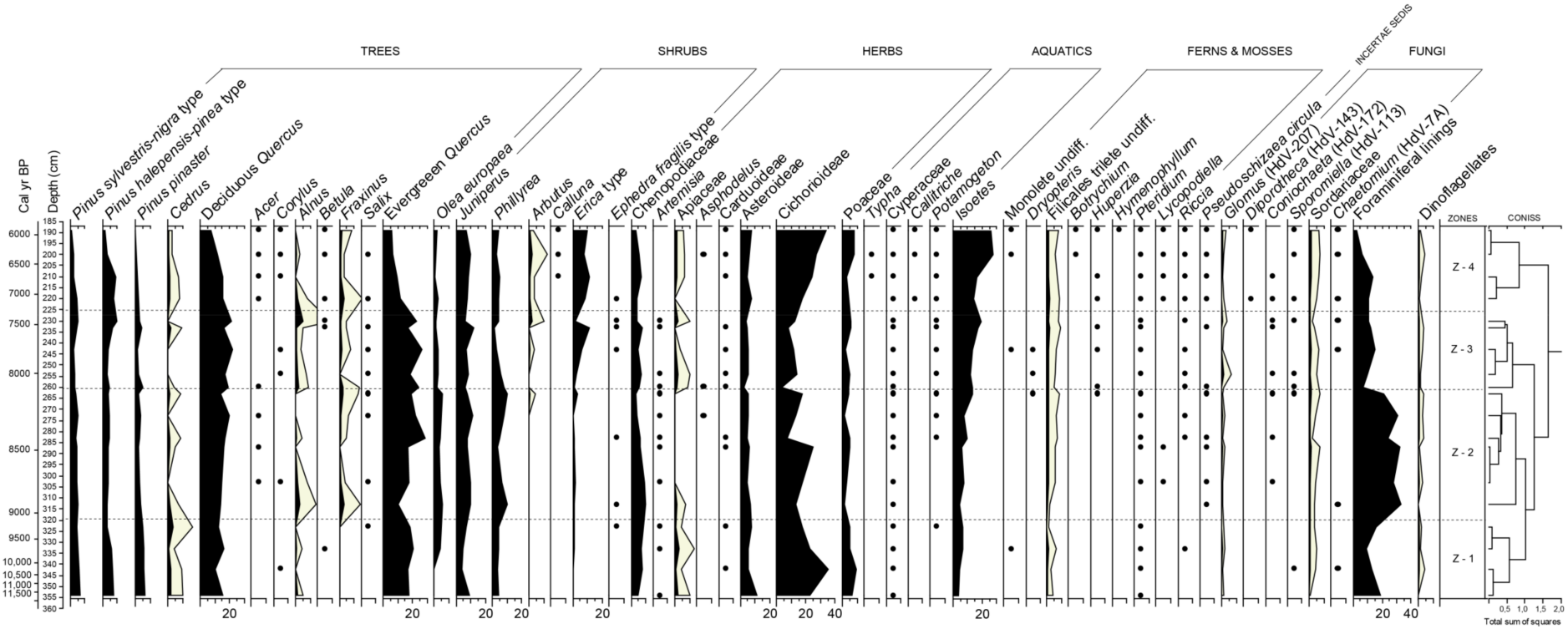

Figure 5. Pollen diagram for the core 19-01 showing trees, shrubs, herbs, aquatics, ferns and mosses, fungi, foraminiferal linings, and dinoflagellates with CONISS zonation vs. depth and age.

4. Discussion

4.1. Geochemical Trends and Events, Sea Level and Palaeoceanographic Changes

Comparison of the evolution of geochemical and sedimentary parameters against regional and global forcings (sea level, climate) (Figure 6), allows us to correlate them and to identify links among the environment, these forcings, and human populations.

The *ca.* 10–6 ka BP period is known as the Holocene Thermal Maximum (HTM) [68–71], a period of warm and humid climate as compared to previous and following periods and only interrupted by a short cooling period known as the 8 ka or the 8.2 ka BP event [72,73] (Figure 6a).

Sea level rose from its previous minimum during the Last Glacial Maximum with maximum rates for the Algarve between 11–8 ka BP (from 9 to 7.4 mm/yr), that decreased between 8–7 ka BP (4.5 mm/yr), and another time from 7 to 6 ka BP (2.0 mm/yr) and fell to 0.7 mm/yr for the 6–5 ka BP period [74]. Coeval to this change, sedimentary records of core 19-01 gradually decrease in grain size (Zr/Rb ratio, Figure 6b) that can be interpreted as the result of deepening (drowning by flooding), increasing distance to the wave base, and the action of coastal currents and sedimentation rates changed accordingly (Figure 6c).

Sea surface temperature decreased in the Gulf of Cádiz [75] and Alborán Sea [76], and this change correlates with the increase in the organic matter content of core 19-01 (Figure 6d).

Weathering proxies are indicative of wet and warm conditions which prevail after 8.2 ka BP (Figure 6e). These conditions are coherent with the alleged characteristics of the HTM and the African Humid Period [77,78]. Stumpf et al. (2011) [78] showed a decrease in the illite/kaolinite ratio and interpreted this as related to a change in dust sources, but it is also coherent with an increase in weathering of the source areas.

The decrease in clastic fraction (Figure 6f) can also be linked to the increase in weathering and the growing water depth. In addition, the continuity of terrestrial influx (Si/Al, Zr/Al, Figure 6g) vs. the gradual increase in organic content and the abrupt and short increase in carbonates around 8.2 ka BP (Ca/Si, Figure 6g) indicate a rise in marine productivity.

However, one of the main features of the geochemical record of core 19-01 is the abrupt change in marine productivity and clastic dynamics and gradual weathering of source areas along with waves/shallow currents. These changes relate to the 8.2 ka BP event.

Thornalley et al. (2009) [79] interpret that there was an abrupt switch from a stratified upper ocean to well-mixed waters around 8.4 ka ago caused by changes in the relations between the subpolar and subtropical gyres. Bazzicalupo et al. (2020) [80] showed from records of the Alborán Sea, that present oceanic gyres system developed around 8 ka ago. Also, models results indicate the changes in oceanic gyres around 8.2 ka BP as being responsible for the present day North Atlantic circulation [81]. Thus, it seems possible that the observed abrupt changes in the geochemical record of core 19-01 can be related to those palaeoceanographic changes, while the gradual ones are interpreted to link to terrestrial climate variations.

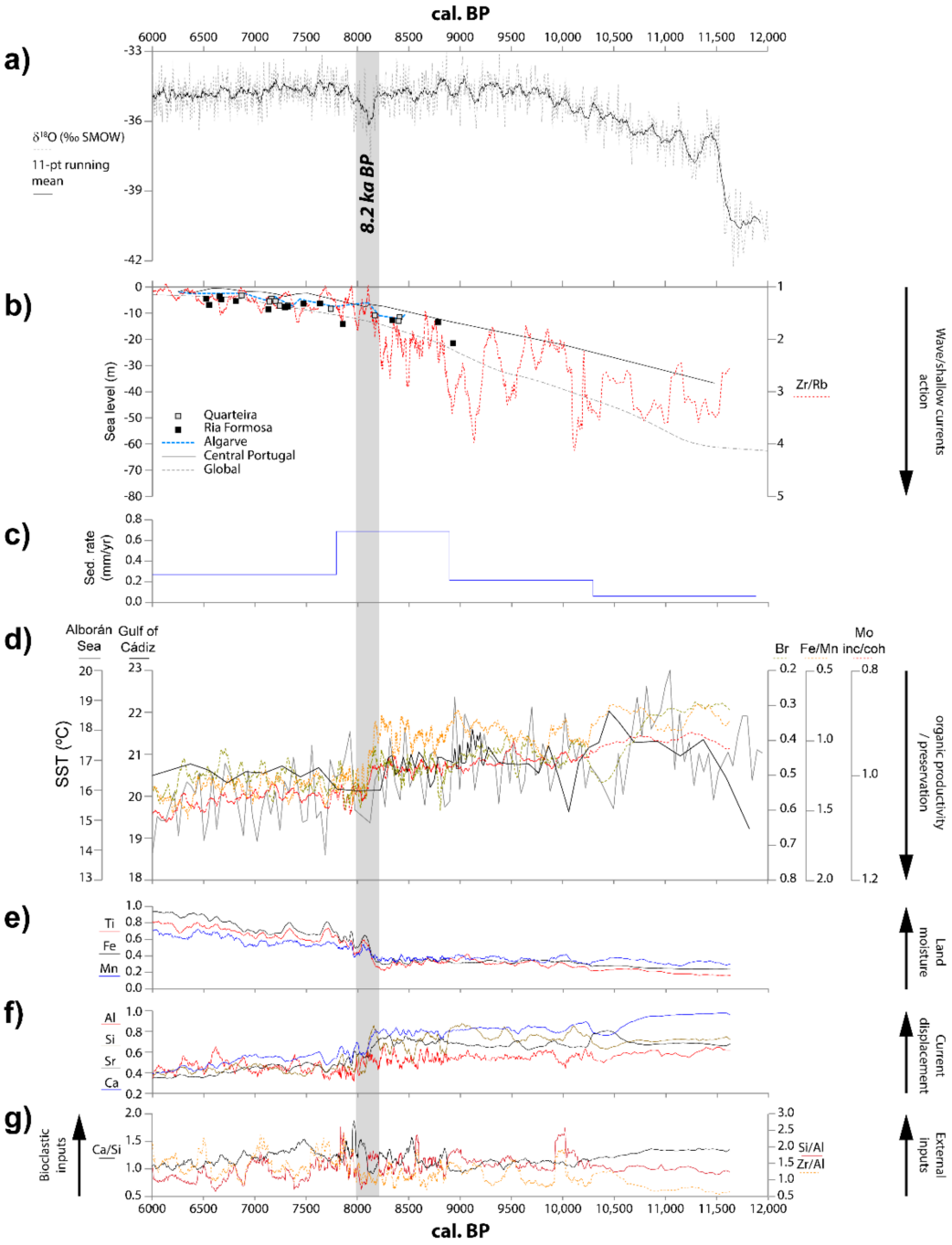

Figure 6. (**a**) Variations in $\delta^{18}O$ in GRIP core [82]; (**b**) sea level changes around SW Portugal (Quarteira [83]; Ria Formosa [84]; Algarve and Central Portugal [74] and global [85] and Zr/Rb ratio (notice the reversed scale); (**c**) sea surface temperature (SST) reconstructions for the Gulf of Cádiz (alkenone Uk37 SST derived for core M39-008 [75]) and Mg/Ca SST derived for the Alborán Sea (ALB2 [76]); (**d**) Ti, Fe, and Mn, weathering proxies, as indicative of land moisture; (**e**) Al, Si, Sr and Ca, representative of clastic sedimentation, serve as proxies for activity of marine currents; (**f**) Ca/Si, carbonate vs. siliciclastics, and Zr/Al and Si/Al, proxies of siliciclastic grains vs. matrix, as indicative of land derived vs. bioclastic (marine) inputs; (**g**) sedimentation rate for core 19-01 for the 12–6 ka BP period.

4.2. Vegetation Trends and Evolution of Coastal Environments

During the Early Holocene, the post-glacial marine transgression was progressively drowning the exposed continental shelf of the southwestern Iberian coast with a rapid sea level rise between *ca.* 13 ka BP and 7–6.5 ka BP, although with different responses depending on the geographic location and topography [27]. Initially, until *ca.* 10 ka BP, the first stages

of the river valleys inundation resulted in pre-estuarine palaeovalleys and transitional areas of fluvial-saltmarsh deposits as the main coastal landscapes [25,86–89]. For this period until *ca.* 9.2 ka BP, the core 19-01 indicates the existence of forests composed of mesophilous trees, and Mediterranean trees and shrubs which defined the onset of the Holocene as a warm phase. Mediterranean and high mountain pines were also present, although in low values, being that the latter (*Pinus sylvestris-nigra* type) may be a reminiscence of the continental climate of the previous glacial period, as reported in other deposits [90]. These conditions have been also inferred in continental deposits in the Guadiana Estuary and the Medina Lagoon, where the presence of open land indicators and high-mountain pines were recorded, respectively [91,92]. In this regard, it has been found that the hydrological response in some Western Mediterranean areas during the Early Holocene maintained prolonged arid conditions, with shallow lake levels followed by an increase of moisture *ca.* 10–9 ka BP [93]. This may have been linked to insolation and seasonality changes due to the orbital variability, the presence of the Laurentide and Fennoscandian ice sheets in the North Atlantic Hemisphere, and a series of ice rafted debris (IRD) provoking immediate ocean surface coolings associated with dry conditions in the Mediterranean region [1,94,95]. Some of these events fall into this period (Figure 7) and two of them appear to have triggered a reaction in the vegetation with a decrease of mesophilous trees and an increase of Asteraceae immediately after 10.3 ka BP, and a retraction of mesophilous and Mediterranean forests with a parallel rise of Mediterranean shrubland and xerophytic taxa after 9.4 ka BP. Diverse records from Greenland show anomalies in the mean $\delta^{18}O$ curves *ca.* 9.95 and 9.3 ka BP interpreted as temperature irregularities, but also to changes in moisture sources and/or transport paths [96,97]. The slight delay in the vegetation reacting to these events indicates that changes in terrestrial landscapes were not immediate.

Regarding the evolution of the coast, the period between *ca.* 10–7 ka BP is also coincident with a phase of intense marine influence due to the marine transgression into the river valleys of the SW Iberian margin, transformed in estuaries by drowning [25,86–89]. As a result, salt marshes developed along the littoral of the Gulf of Cádiz and a landward shift of the boundary between marine and fresh waters took place, with a consequent increase of saline environments [25]. High values of foraminiferal linings were recorded between *ca.* 9.5 to 8 ka BP, probably related to the development of estuaries. From *ca.* 8 ka BP onwards and abrupt drop on the foraminiferal linings gives way to a progressive increase of *Isoetes*, characteristic of seasonal fresh marshland environments [98,99]. The increase of wetland taxa seems to parallel the slight rise of riparian communities registered during this period, which may be a consequence of the influence of the river in the hinterland, as already recorded in other continental cores [86,100].

At *ca.* 10–9 ka BP an abrupt increase in moisture was identified in several lake records of the Western Mediterranean [93], and the progressive expansion and maximum values of oakwoods between *ca.* 10 to 7 ka BP seem to confirm this trend. Despite slight differences in the chronologies, this rise of temperate and Mediterranean forest taxa is also registered in other marine cores drilled in the Atlantic margin of southwestern Iberia [101–103], as well as in some continental deposits of this area [91].

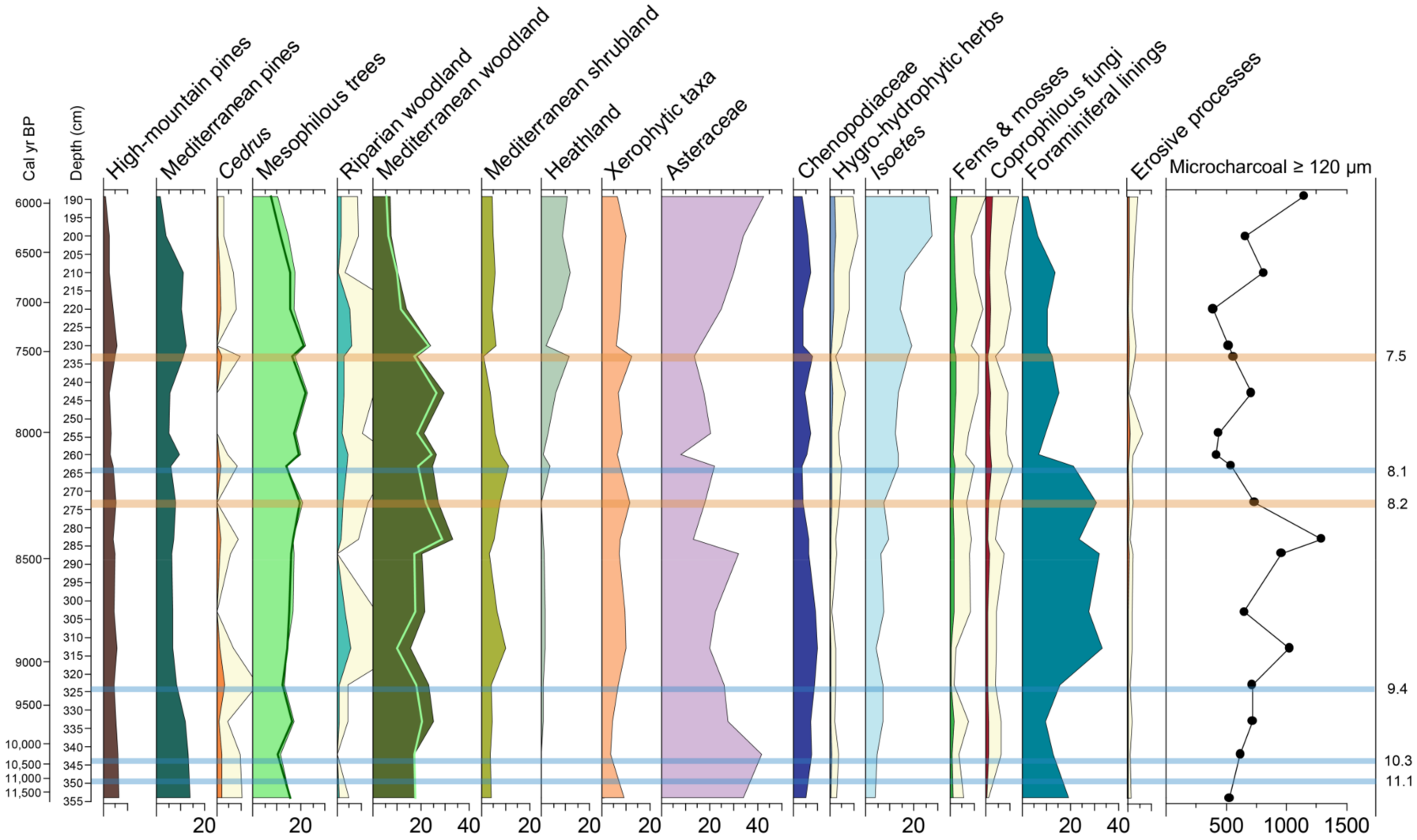

Figure 7. Synthetic diagram of the main ecological groups and taxa expressed in percentages. The dark green line plotted against the Mesophilous trees represents deciduous *Quercus* values, while the light green line plotted against the Mediterranean woodland shows evergreen *Quercus* values. Microcharcoals are expressed in concentrations (particles/gr of dry sediment). Blue lines correspond to the IRD events (Bond et al., 1997) with a clear impact in the vegetation identified in the core 19-01, while orange lines highlight aridity crises.

During this period, two peaks of microcharcoals were recorded and interpreted as episodes of increased regional wildfires at 8.8 and 8.4 ka BP (Figure 7). Several forest contractions were also identified at different points and with diverse characteristics but it is noteworthy to highlight two episodes. At 8.2 ka BP there is an increase of xerophytic elements and afterwards an abrupt drop of the forest taxa took place, culminating with low values of mesophilous/Mediterranean trees and a rise of Asteraceae *ca.* 8.1 ka BP. Greenland ice cores reflect well-defined anomalies in the period between 8.4–8 ka BP with very low values of δ18O around 8.2 ka BP [97]. Although its origins remain unclear, the 8.2 ka BP event has been linked to a fresh water influx into the North Atlantic that would have provoked changes in temperatures and thermohaline circulation and thus, in moisture availability [1,104]. Indeed, the Medina Lagoon record shows a lake-level decrease for the period between *ca.* 8.5–7.8 ka BP, which has been related to global climatic instability centered on 8.2 ka BP, concluding in a desiccation phase [105]. Events of forest decrease were also recorded in the SW Atlantic margin between *ca.* 8.6–8 ka BP, as well as in the Alborán Sea between *ca.* 8.3–8 ka BP [101–103,106,107]. In continental deposits, some forest setbacks and expansion of open-ground taxa were recorded in the Guadiana Valley and the Medina Lagoon at *ca.* 7.8 and 8.2 ka BP, respectively [91,108]; however, several sequences do not mirror any vegetal changes for this period [15,109].

Another important crisis was also identified in the GeoB235-19-01 core at *ca.* 7.5 ka BP, defined by a visible peak of xerophytes and an abrupt drop of mesophilous trees, riparian woodland, and Mediterranean woodland and shrubland, pointing to a rapid decrease of moisture availability (Figures 6e and 7). Diverse episodes of forest contractions were identified between 7.5 and 7 ka BP in different cores of the Atlantic Iberian Margin and the Alborán Sea, as well as in continental sequences [91,101–103,106,107,109]. Diverse palaeorecords from SE Iberia suggest changes towards increased aridity between 7.8–7.3 ka BP [110].

Regarding the coastal evolution, the core 19-01 recorded the maximum sea level rise rates for the Algarve between 11–7 ka BP, but in most of the estuaries located in this area (Alvor, Alcantarilha, Quarteira, Carcavai, Tinto & Odiel, Guadalete) the maximum flooding of the river valleys was registered at *ca.* 7–6 ka BP, resulting in the development of open estuaries, inundated channel banks, tidal flats, and even the landward migration of estuarine barriers [25,86–89]. The fluctuation between marine *vs* freshwater markers recorded in the core 19-01 seems to reflect the marine pulses and the diverse evolution of littoral features and edaphic conditions, depending on factors such as the accommodation space of the river valleys. During this millennium, mesophilous and Mediterranean woodland progressively decrease, while Mediterranean shrubland seem to stabilize at the same time that heaths start a stepwise expansion from this point onwards. An important increase of Cichorioideae occur *ca.* 6 ka BP, correlating the rise of *Isoetes* and hygro-hydrophytic herbs. The ambiguous significance of Cichorioideae makes it difficult to understand this episode, and its presence may suggest an important development of marsh/wetland communities, or either the development of a semi-open landscape paralleling the expansion of shrublands to the detriment of forests.

After *ca.* 6 ka BP, rates of sea level rise fell to 0.7 mm/yr in the Algarve [74], while in most of the estuaries of this area rates are of *ca.* 2.6 mm/yr and oscillations below 1 m defined the last 5000 years [27,111,112]. Some coastal elements like lagoons, spits, and barriers developed during this period [113].

4.3. Human Groups in Dynamic Littoral Habitats

The rapid sea level rise occurring from *ca.* 13 to 7 ka BP was one of the main influential factors affecting the evolution of the coastal morphology and, therefore, human settlements. It is assumed that if the currently known Mesolithic sites were distributed along the coast, other hunter-gatherer occupations may have existed in the exposed continental shelf before its flooding due to marine transgression, which in that case may have been erased by the sea. The absence of any human settlement previous to *ca.* 9 ka BP in the studied

area, with exception of one date in Barranco das Quebradas [13], is a clear example of the consequences of the sea level rise in this region.

From *ca*. 9 ka BP onwards, all the preserved Mesolithic sites are located at or above 50 m asl, except Castelejo and Palmones (supplementary material), and with direct access to the sea, considering the coastline at that time (Figure 8). The lack of data in the littoral of the Gulf of Cádiz during this time span is critical, but it is especially dramatic in the central and eastern sector. The fact that most of the preserved sites are located in the cliffy area could be explained by a greater spatial impact of the sea level rise on the coastal plains at that time opened to the sea, since most of the spits and barriers developed after *ca.* 6 ka BP [27,111–113].

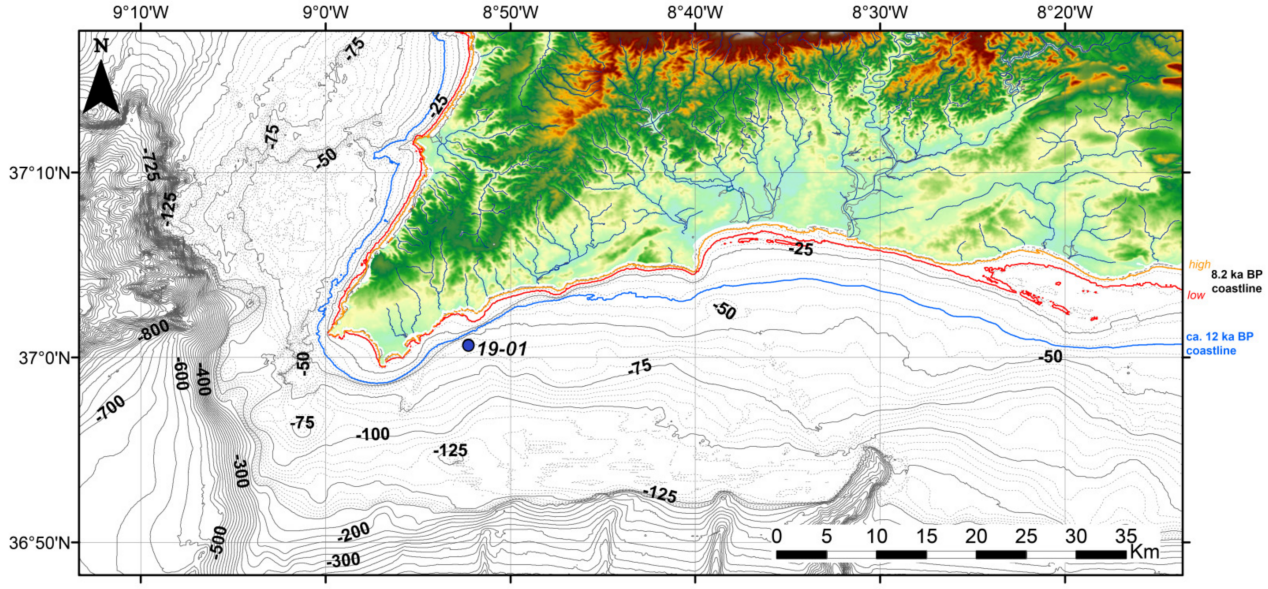

Figure 8. Digital terrain model map and bathymetry of the westernmost Algarve coast. Blue line indicates the coastline *ca*. 12 ka BP, red line shows the lowest possible coastline *ca*. 8. 2 ka BP, and yellow line situates the highest possible coastline *ca*. 8.2 ka BP. Blue dot represents the core 19-01. (Data source for bathymetry: EMODnet, https://www.emodnet-bathymetry.eu/ (accessed on 14 March 2021), for elevation: EU-DEM v.1.1, https://land.copernicus.eu/imagery-in-situ/eu-dem/eu-dem-v1.1 (accessed on 14 March 2021)).

For the period between *ca.* 9–7.5 ka BP, recent palaeodemographic studies propose a steady growth in population reflected in a concentration of archaeological sites in Central-South Portugal (Muge and Sado estuaries) and across the Algarve, although here in a more dispersed pattern [114]. Most of the sites concentrated in Western Algarve are shell-middens and with exemption of Vale Boi, where a human tooth dating of Mesolithic but without a funerary context was described [16], all the occupations in this region are seasonal camps focused on the collection of local resources, mainly marine food but also flint material [13]. Some hypotheses correlate these sites with the existence of some (semi)permanent basecamps on which they would depend and that would have similar characteristics to those from the Sado and Tejo estuaries, with elaborated habitational structures, human burials, and broad-spectrum subsistence strategies [6,12,115,116]. However, no (semi)permanent basecamps have been found in the Algarve region yet, and it seems to be a hard task considering the high level of human impact of this area during historic times. Regarding the eastern sector of the Gulf of Cádiz, environmental differences, and the specific cultural trajectories in the "Alborán territory" [8], the nearest area where most of the pre-Neolithic sites are located, prevent us from establishing any comparison between archaeological sites of both zones.

Some authors consider that major changes in the social, technological, economic, and in settlement patterns of hunter-gatherer groups did not occur with the transition from

the Late Pleistocene to the Holocene, but in relation to the 8.2 ka BP event. An example would be the development of the complex shell-midden basecamps located in inland areas following the course of the Tejo and Sado Rivers, as opposed to the seasonal shell-middens located in the Algarve coast. This change of settlement patterns is explained as the result of a decline in the availability of the marine resources due to the joint action of a drop in the upwelling intensity together with an increased aridity *ca.* 8.2 ka BP [116]. This would have made the palaeoestuaries of these rivers stable resource-rich brackish environments, unlike the coastal unstable ecosystems adversely affected by this episode [116]. Likewise, results from the Pena d'Agua rock-shelter show important changes in the acquisition of raw material and technological features, which would be explained by modifications in mobility patterns from residential to logistic as an adaptive response to changing environments from 8.2 ka BP onwards [117]. Considering this hypothesis, these changes may have accelerated the confluence of human groups to settle in areas with stable and available resources, resulting in a (semi)sedentary pattern and social complexity [116–118]. However, there is no sign of the impact of the 8.2 ka BP event in the SW Atlantic Iberian margin in terms of settlement patterns. Notwithstanding, the bias caused by the lack of information needs more research in the study area to discern whether the seasonality of these sites reflect important regional differences, or if it is related to the existence of some (semi)permanent undiscovered basecamps.

Regarding the diet, not only shell-middens from Western Algarve display a specialization in the exploitation of marine resources, but also the seasonal occupation of Palmones revealed an intense gathering of shellfish [15]. Isotopic analysis of the Vale Boi teeth showed that, although marine resources were a prominent element, the diet of these Mesolithic groups was based on a mix of terrestrial and aquatic resources [12]. However, there may have been important differences between sites, because isotopic data from the Sado shell-middens corroborated frequencies of marine diet *ca.* 25% [119], while in the Muge area the marine diet is above 50% [120].

In the occidental area of the Algarve, topshells were the most abundant species consumed during the Early Mesolithic, while limpets and gooseneck barnacles were preferred during the Late Mesolithic and Early Neolithic [121]. A reduction in the size of the shellfish collected was also identified in the transition from Mesolithic to Neolithic at Vale Boi, Rocha das Gaivotas, and Armação Nova, and it was considered a consequence of overexploitation [12] or a decrease in the foraging efficiency [121]. However, in some Mediterranean areas such as the Pego palaeolagoon, a reduction of lagoon bivalve size during the Late Mesolithic has been observed, related to a decrease in resource productivity [122]. Despite this there was gently increase in ocean organic productivity linked to the slow overall cooling of the waters during the Mid Holocene, the warmer climate during the Holocene Thermal Maximum caused a weakening of the coastal upwelling, briefly interrupted during the short cooling episodes [79]. This alteration in the coastal palaeoproductivity suggests that the modification in consumption patterns and the size decrease of shellfish in SW Iberian sites may have been a consequence of these environmental alterations rather than being caused by cultural factors.

Commonly, the expansion of the Neolithic in both the western and eastern sectors of the Gulf of Cádiz is considered to have occurred around 7.5 ka BP [9,12]. Corresponding to the period, different sequences reflect an aridity crisis affecting the vegetation of the SW Atlantic Iberian coast and the Alborán Sea [91,101–103,106,107,109] and the geochemistry dataset reflects a decrease of land moisture (Figure 6e). Some Mesolithic sites exhibit layers of Neolithic occupations (Castelejo, Barranco das Quebradas, Rocha das Gaivotas, Vale Boi, Palmones), although with hiatuses of several hundred years. The existence of several seasonal camps (Alcalar 7, Ribeira de Alcantarilha, Vale Santo I, Padrão, El Retamar) suggests the maintenance of previous subsistence strategies until this period. However, Neolithic times also involve new settlement patterns with sites located near rivers, shell deposits thinner than those in the Mesolithic, and caves. Only two sites suggest clear sedentary occupation (Castelo Belinho, Campo de Hockey) and the presence of seasonal

camps reveals that the mobility was still key in the provisioning of different resources. Although the aim of this paper is not to discuss the origins of the Neolithic in the study area, the coexistence of previous (Mesolithic) and new (Neolithic) settlement patterns would be coherent with the idea of an integration of the two populations, rather than with the disappearance of the hunter-gatherer way of life [120].

It is noteworthy to mention that except the pre-existing sites and some exceptions such as Praia do Forte Novo, El Retamar, and Campo de Hockey, all the Neolithic sites are located a few kilometres inland. Some changes in dietary habits regarding aquatic resources may be linked to this new settlement pattern, with the increased consumption of cockles and clams [121] typical from transitional brackish environments (rías), in contrast to the rocky-like shellfish preferred during the Mesolithic. Some ideas of what may lie behind this change in settlement patterns are:

- Different populations would have a different perception of the same habitat, so they develop preferences for settling in distinct areas.
- The maximum flooding of some river valleys would have forced human groups to settle in areas less close to the coastline. It should be also considered that archaeological sites located in the mouth of these rivers could have been buried or destroyed after this flooding episode and only those located in inland areas are preserved.
- The weakening of the coastal upwelling during the Holocene Thermal Maximum may have caused a displacement toward areas with more stable resource availability, like what occurred in the Tejo and Sado estuaries *ca*. 8.2–8 ka BP. Due to the bias in the preservation of Mesolithic sites in the study area, it is not possible to delineate to what extent this would have affected Mesolithic populations and to compare it to the Neolithic groups.
- The aridity crisis reflected in the vegetation *ca*. 7.5 ka BP and recorded in other sequences *ca*. 7.5–7 ka BP may have led human groups to settle in areas more suitable for livestock and/or agriculture activities with available freshwater sources. One might speculate whether the aridity phase experienced during this period might have influenced the adoption of new subsistence strategies.

Regarding the resource exploitation and subsistence strategies, the introduction of a farming economic system resulted in a major dietary shift towards terrestrial food during this transitional period [123]. In relation to the agricultural practices, the first evidences were dated *ca.* 7.5–7 ka BP in Eastern Andalusia and Central-South Portugal, while there is not any direct evidence of their origins in the Occidental Andalusia and the Algarve area [124]. Livestock and grazing activities have direct testimony in zooarchaeological material. With respect to palynology, anthropogenic indicators are most likely to be identified in continental and especially archaeological deposits than in marine cores. However, the first manifestations of agricultural activities are only documented *ca.* 6 ka BP in areas with previous and important Mesolithic occupations [124].

In relation to the preservation of human settlements, the lack of data in the central coast of the Gulf of Cádiz for both Mesolithic and Neolithic periods must be considered. Some archaeological sites and material identified in the surface [3] are ascribed to the Early Neolithic, but the absence of systematic excavations and datings makes it presently impossible to shed light on the evolution of human groups during this time span. However, these settlements display a similar pattern compared with those of the Algarve, located close to the coast but some kilometers inland and near the Tinto, Odiel, Guadalquivir, and Guadalete rivers. An important issue to consider is related to the several high energy wave events that have been identified in this area during this period. In the Guadalquivir estuary, several high energy events were identified between 9.9–9.2 ka BP and 8.2–7.8 ka BP, some of them of unclear origin, some identified as storms, and one of them at 9.1 ka BP of tsunamigenic origins, while *ca.* 7–6.8 ka BP a palaeotsunami occurred [109,125]. The westernmost Algarve area was also hit by a high energy wave event, only identified in the Alvor estuary *ca.* 6.4 ka BP [86]. Thus, not only the sea level rise but the hazardous nature of the coastal plain in this region, which seems to be constantly subject to these

extreme events as well as affected by subsidence, may hamper the detection of potential archaeological sites.

5. Conclusions

This paper presents a new palaeonvironmental dataset that contributes to a better understanding of the evolution of coastal landscapes in the littoral of the Gulf of Cádiz. The multi-proxy approach combining palynological, geochemical, and sedimentological data has provided a framework to better contextualize human occupations in SW Iberia during the Early-Mid Holocene (*ca*. 12–6 ka BP). A review of the state of the art regarding the archaeological research in this area was done considering the known archaeological sites with a reliable chronological control, which revealed an important lack of data. Some of our most important conclusions can be summed up as follows:

- The onset of the Holocene is characterized by an increase in temperature, but weak continental conditions seem to remain until *ca.* 10 ka BP. Between *ca.* 10–7 ka BP there is an increase of forest values composed of mesophilous and Mediterranean taxa reflecting a rise of moisture, after which an important decrease in the forest cover occurred followed by a stepwise rise of heathlands *ca.* 7 ka BP.
- Peaks of aridity indicators were identified at 8.2 and 7. 5 ka BP. The 8.2 ka BP event seems to affect vegetation with some delay, while the 7.5 ka BP event has an immediate impact in different taxa.
- Changes detected in the geochemical record at *ca*. 8.2 ka BP seem to lead to abrupt palaeoceanographic modifications, but smooth gradual terrestrial changes. The first were responsible of modifications in the current system that could have affected the coastal productivity. The 7.5 ka BP event mirror a decrease in land moisture availability.
- Holocene sea level rise shaped the coastal morphology and influenced the settlement patterns of human groups in both Mesolithic and Early Neolithic times, as well as the preservation of archaeological sites. High energy events and the subsidence to which certain areas are subjected have hampered the preservation of any potential remain.
- Subsistence strategies based on the aquatic resource exploitation were common to hunter-gatherer groups during the Mesolithic, but also during the early stages of the Neolithic.
- Only seasonal camps were identified among the Mesolithic sites in the study area, contrary to the (semi)permanent sites in South-Central Portugal. This may be tentatively interpreted as an effect of the lack of data due to the marine transgression or different regional patterns.
- Mesolithic sites are located along the coastline with direct access to the sea. Although some of them persist during the Early Neolithic, in this period most of the sites are located near rivers some kilometers inland. Several hypotheses were presented to understand this change in settlement patterns.
- Changes in dietary habits and the characteristics of some shellfish species during the Late Mesolithic/Early Neolithic seem to have been related to environmental changes rather than to cultural preferences or human overexploitation.
- There are no clear evidences of the origins of agriculture in the studied area, which may be due to an archaeological bias or a consequence of a later adoption of this practice.

Supplementary Materials: The following are available online at https://zenodo.org/deposit/4646170.

Author Contributions: Conceptualization, methodology, software, validation, formal analysis, investigation, data curation, and writing—original draft preparation, C.V.-P. and J.I.S.; writing—review and editing, C.V.-P., J.I.S., J.A.L.-S., G.-C.W., K.R.; resources, supervision, K.R.; project administration, K.R. and G.-C.W.; funding acquisition, K.R. and G.-C.W. All authors have read and agreed to the published version of the manuscript.

Funding: This research was funded by the Deutsche Forschungsgemeinschaft (DFG, German Research Foundation)—Projektnummer 57444011, SFB 806—and by the Fundação para a Ciência e Tecnologia (FCT)—Project OnOff, PTDC/CTAGEO/28941/2017.

Institutional Review Board Statement: Not applicable.

Informed Consent Statement: Not applicable.

Acknowledgments: The authors are grateful to the research and technical crew under the command of Captain Hammacher from RV METEOR–M152 and to Melles (University of Cologne) who kindly facilitated access to an ITRAX core scanner for XRF analysis.

Conflicts of Interest: The authors declare no conflict of interest.

References

1. Bond, G.; Kromer, B.; Beer, J.; Muscheler, R.; Evans, M.N.; Showers, W.; Hoffmann, S.; Lotti-Bond, R.; Hajdas, I.; Bonani, G. Persistent Solar Influence on North Atlantic Climate during the Holocene. *Science* **2001**, *294*, 2130–2136. [CrossRef] [PubMed]
2. Zilhão, J. Radiocarbon Evidence for Maritime Pioneer Colonization at the Origins of Farming in West Mediterranean Europe. *Proc. Natl. Acad. Sci. USA* **2001**, *98*, 14180–14185. [CrossRef] [PubMed]
3. Muñoz, J.R. Las Industrias Líticas Del Neolítico En Andalucía, Sus Implicaciones Espaciales y Económicas. *Zephyrus* **1988**, *41*, 113–148.
4. Massieu, M.; Socas, D.M. Los Inicios Del Neolítico En Andalucía. Entre La Tradición y La Innovación. *MENGA Rev. Prehist. Andal.* **2013**, *4*, 103–129.
5. Manen, C.; Marchand, G.; Carvalho, A. *Le Néolithique Ancien de La Péninsule Ibérique: Vers Une Nouvelle Évaluation Du Mirage Africain?* Société Préhistorique Française: Avignon, France, September 2004; Volume 3, pp. 133–151.
6. Carvalho, A.F. Le passage vers l'Atlantique: Le processus de néolithisation en Algarve (sud du Portugal). *L'Anthropologie* **2010**, *114*, 141–178. [CrossRef]
7. Borja, P.G.; Tortosa, J.E.A.; Aubán, J.B.; Pardo, J.F.J. Nuevas perspectivas sobre la neolitización en la cueva de Nerja (Málaga-España): La cerámica de la sala del vestíbulo. *Zephyrus Rev. Prehist. Arqueol.* **2010**, *66*, 109–132.
8. Linstädter, J.; Medved, I.; Solich, M.; Weniger, G.-C. Neolithisation Process within the Alboran Territory: Models and Possible African Impact. *Quat. Int.* **2012**, *274*, 219–232. [CrossRef]
9. Martín-Socas, D.; Camalich Massieu, M.D.; Herrero, J.L.C.; Rodríguez-Santos, F.J. The Beginning of the Neolithic in Andalusia. *Quat. Int.* **2017**, *470*, 451–471. [CrossRef]
10. Fregel, R.; Méndez, F.L.; Bokbot, Y.; Martín-Socas, D.; Camalich-Massieu, M.D.; Santana, J.; Morales, J.; Ávila-Arcos, M.C.; Underhill, P.A.; Shapiro, B.; et al. Ancient Genomes from North Africa Evidence Prehistoric Migrations to the Maghreb from Both the Levant and Europe. *Proc. Natl. Acad. Sci. USA* **2018**, *115*, 6774–6779. [CrossRef]
11. Valdiosera, C.; Günther, T.; Vera-Rodríguez, J.C.; Ureña, I.; Iriarte, E.; Rodríguez-Varela, R.; Simões, L.G.; Martínez-Sánchez, R.M.; Svensson, E.M.; Malmström, H.; et al. Four Millennia of Iberian Biomolecular Prehistory Illustrate the Impact of Prehistoric Migrations at the Far End of Eurasia. *Proc. Natl. Acad. Sci. USA* **2018**, *115*, 3428–3433. [CrossRef]
12. Carvalho, A.F. A Neolitização do Portugal Meridional: Os Exemplos do Maciço Calcário Estremenho e do Algarve Ocidental. Ph.D. Thesis, University of Algarve, Faro, Portugal, 2007.
13. Valente, M.J.; Carvalho, A.F. Recent Developments in Early Holocene Hunter-Gatherer Subsistence and Settlement: A View from South-Western Iberia. In *Mesolithic Horizons, Proceedings of the Seventh International Conference on the Mesolithic in Europe, Belfast, Ireland, 2005*; McCartan, S., Schulting, R., Warren, G., Woodman, P., Eds.; Oxbow Books: Belfast, Ireland, 2009; pp. 312–317.
14. Ramos-Muñoz, J.R.; Castañeda, V.C. *Excavación en el Asentamiento Prehistórico del Embarcadero del río Palmones (Algeciras, Cádiz): Una Nueva Contribución al Estudio de las Últimas Comunidades Cazadoras y Recolectoras*; Servicio de Publicaciones de la Universidad de Cádiz y Ayuntamiento de Algeciras: Cádiz, Spain, 2005.
15. Uzquiano, P.; Ruiz-Zapata, B.; Gil-Garcia, M.J.; Vijande, E.; Ramos-Muñoz, J.; Cantillo, J.J.; Lazarich, M.; Bejarano, D.; Montañés, M. Mid-Holocene Palaeoenvironmental Record from the Atlantic Band of Cádiz (SW Spain) Based on Pollen and Charcoal Data. *Quat. Int.* **2020**. [CrossRef]
16. Peyroteo-Stjerna, R. Chronology of the Burial Activity of the Last Hunter-Gatherers in the Southwestern Iberian Peninsula, Portugal. *Radiocarbon* **2020**, 1–35. [CrossRef]
17. Rocha, L. A praia do Forte Novo. Um sítio de produção de sal na costa Algarvia? *Setúbal Arqueológica* **2013**, *14*, 225–232.
18. Ramos-Muñoz, J. La Ocupación Prehistórica de La Campiña Litoral y Banda Atlántica de Cádiz. Aproximación al Estudio de Las Sociedades Cazadoras-Recolectoras, Tribales-Comunitarias y Clasistas Iniciales. *MENGA Rev. Prehist. Andal.* **2010**, *66*, 278–279. [CrossRef]
19. Stipp, J.J.; Timers, M.A. Datación radiométrica. In *El Asentamiento de El Retamar (Puerto Real, Cádiz): Contribución al Estudio de la Formación Social Tribal y a los Inicios de la Economía de Producción en la Bahía de Cádiz*; Ramos, L., Ed.; Servicio de Publicaciones de la Universidad de Cádiz y Ayuntamiento de Algeciras: Cádiz, Spain, 2002; pp. 169–174.

20. Vijande, E. El Poblado de Campo de Hockey (San Fernando, Cádiz): Resultados Preliminares y Líneas de Investigación Futuras Para El Conocimiento de Las Formaciones Sociales Tribales En La Bahía de Cádiz (Tránsito V-IV Milenios A.N.E.). *Revista Atlántica-Mediterránea de Prehistoria y Arqueología Social* **2009**, *11*, 265–284.
21. Vijande, E.; Domínguez-Bella, S.; Duarte, J.J.C.; López, J.M.; Tocino, A.B. Social Inequalities in the Neolithic of Southern Europe: The Grave Goods of the Campo de Hockey Necropolis (San Fernando, Cádiz, Spain). *Comptes Rendus Palevol* **2015**, *14*, 147–161. [CrossRef]
22. Muñoz, L.P.S.-B.; Vila, E.V.; Salvador, Á.R.; Aguilera, I.A.; Bonilla, M.D.-Z.; Márquez, A.M.; Domínguez-Bella, S.; Muñoz, J.R.; López, M.C.B. Possible Interpersonal Violence in the Neolithic Necropolis of Campo de Hockey (San Fernando, Cádiz, Spain). *Int. J. Paleopathol.* **2019**, *27*, 38–45. [CrossRef]
23. García-Rivero, D.; Taylor, R.; Umbelino, C.; Price, T.D.; García-Viñas, E.; Bernáldez-Sánchez, E.; Pérez-Jordà, G.; Peña-Chocarro, L.; Barrera-Cruz, M.; Gibaja-Bao, J.F.; et al. The Exceptional Finding of Locus 2 at Dehesilla Cave and the Middle Neolithic Ritual Funerary Practices of the Iberian Peninsula. *PLoS ONE* **2020**, *15*, e0236961. [CrossRef]
24. Ramos, A.; Fernández, O.; Terrinha, P.; Muñoz, J.A. Extension and Inversion Structures in the Tethys–Atlantic Linkage Zone, Algarve Basin, Portugal. *Int. J. Earth Sci.* **2016**, *105*, 1663–1679. [CrossRef]
25. Dabrio, C.J.; Zazo, C.; Goy, J.L.; Sierro, F.J.; Borja, F.; Lario, J.; González, J.A.; Flores, J.A. Depositional History of Estuarine Infill during the Last Postglacial Transgression (Gulf of Cadiz, Southern Spain). *Mar. Geol.* **2000**, *162*, 381–404. [CrossRef]
26. Hernández-Molina, F.J.; Llave, E.; Stow, D.A.V.; García, M.; Somoza, L.; Vázquez, J.T.; Lobo, F.J.; Maestro, A.; Díaz del Río, V.; León, R.; et al. The Contourite Depositional System of the Gulf of Cádiz: A Sedimentary Model Related to the Bottom Current Activity of the Mediterranean Outflow Water and Its Interaction with the Continental Margin. *Deep. Sea Res.* **2006**, *53*, 1420–1463. [CrossRef]
27. Zazo, C.; Dabrio, C.J.; Goy, J.L.; Lario, J.; Cabero, A.; Silva, P.G.; Bardají, T.; Mercier, N.; Borja, F.; Roquero, E. The Coastal Archives of the Last 15 Ka in the Atlantic-Mediterranean Spanish Linkage Area: Sea Level and Climate Changes. *Quat. Int.* **2008**, *181*, 72–87. [CrossRef]
28. Kottek, M.; Grieser, J.; Beck, C.; Rudolf, B.; Rubel, F. World Map of the Köppen-Geiger Climate Classification Updated. *Meteorol. Z.* **2006**, 259–263. [CrossRef]
29. AEMET. *Atlas Climático Ibérico—Iberian Climate Atlas*; Agencia Estatal de Meteorología: Madrid, Spain, 2011; ISBN 978-84-7837-079-5.
30. Espírito-Santo, D.; Capelo, J.; Neto, C.; Pinto-Gomes, C.; Ribeiro, S.; Canas, R.Q.; Costa, J.C. Lusitania. In *The Vegetation of the Iberian Peninsula*; Loidi, J., Ed.; Springer International Publishing: Cham, Switzerland, 2017; Volume 2, pp. 35–82.
31. Rivas-Martínez, S. Bioclimatología, Biogeografía y Series de Vegetación En Andalucía Occidental. *Lagascalia* **1988**, *15*, 91–119.
32. Rivas-Martínez, S.; Lousa, M.; Día, T.E.; Fernández.-González, F.; Costa, J.C. La Vegetación Del Sur de Portugal (Sado, Alemtejo y Algarve). *Itinera Geobot.* **1990**, *3*, 5–126.
33. Rivas-Martínez, S.; Fernández-González, F.; Loidi, J.; Lousa, M.; Penas, A. Syntaxonomical Checklist of the Vascular Plant Communities of Spain and Portugal to Association Level. *Itinera Geobot.* **2001**, *14*, 5–341.
34. Loidi, J.; Biurrun, I.; Campos, J.A.; García-Mijangos, I.; Herrera, M. A Survey of Health Vegetation of the Iberian Peninsula and Northern Morocco: A Biogeographic and Bioclimatic Approach. *Phytocoenologia* **2007**, *37*, 341–370. [CrossRef]
35. Martínez, S.R.; Valdés, E.; Costa, M.; Castroviejo, S. Vegetación de Doñana (Huelva, España). *Lazaroa* **1980**, *2*, 5–190.
36. Marcenò, C.; Guarino, R.; Loidi, J.; Herrera, M.; Isermann, M.; Knollová, I.; Tichý, L.; Tzonev, R.T.; Acosta, A.T.R.; FitzPatrick, Ú.; et al. Classification of European and Mediterranean Coastal Dune Vegetation. *Appl. Veg. Sci.* **2018**, *21*, 533–559. [CrossRef]
37. Rivas-Martínez, S.R.; Belmonte-López, M.D.B. Sobre el orden Agrostietalia castellanae. *Lazaroa* **1985**, 417–420.
38. Calvert, S.E.; Pedersen, T.F. Chapter Fourteen Elemental Proxies for Palaeoclimatic and Palaeoceanographic Variability in Marine Sediments: Interpretation and Application. In *Developments in Marine Geology*; Hillaire–Marcel, C., De Vernal, A., Eds.; Proxies in Late Cenozoic Paleoceanography; Elsevier: Amsterdam, The Netherlands, 2007; Volume 1, pp. 567–644.
39. Calib 8.2. Available online: http://calib.org/calib/calib.html (accessed on 18 March 2021).
40. Heaton, T.J.; Köhler, P.; Butzin, M.; Bard, E.; Reimer, R.W.; Austin, W.E.N.; Ramsey, C.B.; Grootes, P.M.; Hughen, K.A.; Kromer, B.; et al. Marine20—The Marine Radiocarbon Age Calibration Curve (0–55,000 Cal BP). *Radiocarbon* **2020**, *62*, 779–820. [CrossRef]
41. Martins, J.M.M.; Soares, A.M.M. Marine Radiocarbon Reservoir Effect in Southern Atlantic Iberian Coast. *Radiocarbon* **2013**, *55*, 1123–1134. [CrossRef]
42. Soares, A.M.M. The ^{14}C Content of Marine Shells: Evidence for Variability in Coastal Upwelling off Portugal during the Holocene. In *Isotope Techniques in the Study of Past and Current Environmental Changes in the Hydrosphere and the Atmosphere*; International Atomic Energy Agency: Vienna, Austria, 1993; pp. 471–485.
43. Soares, A.M.M.; Dias, J.M.A. Coastal Upwelling and Radiocarbon—Evidence for Temporal Fluctuations in Ocean Reservoir Effect off Portugal During the Holocene. *Radiocarbon* **2006**, *48*, 45–60. [CrossRef]
44. Soares, A.M.M.; Martins, J.M.M. Radiocarbon Dating of Marine Shell Samples. The Marine Radiocarbon Reservoir Effect of Coastal Waters off Atlantic Iberia during Late Neolithic and Chalcolithic Periods. *J. Archaeol. Sci.* **2009**, *36*, 2875–2881. [CrossRef]
45. Soares, A.M.M.; Martins, J.M.M. Radiocarbon Dating of Marine Samples from Gulf of Cadiz: The Reservoir Effect. *Quat. Int.* **2010**, *221*, 9–12. [CrossRef]
46. Reimer, R.W.; Reimer, P.J. An Online Application for ΔR Calculation. *Radiocarbon* **2017**, *59*, 1623–1627. [CrossRef]

47. López-Sáez, J.A.; Geel, B.; Sánchez, M. *Aplicación de Los Microfósiles No Polínicos En Palinología Arqueológica, Contributos das Ciencias e das Tecnologias para a Arqueologia da Península Ibérica, Proceedings of the 3° Congresso de Arqueología Peninsular, Vila Real, Portugal, 1999*; Oliveira, V., Ed.; UTAD: Vila Real, Portugal, 2002.
48. Miola, A. Tools for Non-Pollen Palynomorphs (NPPs) Analysis: A List of Quaternary NPP Types and Reference Literature in English Language (1972–2011). *Rev. Palaeobot. Palynol.* **2012**, *186*, 142–161. [CrossRef]
49. Moore, P.D.; Webb, J.A.; Collinson, M.E. *Pollen Analysis*; Blackwell Science: Oxford, UK, 1991; ISBN 978-0-86542-895-9.
50. Pals, J.P.; Van Geel, B.; Delfos, A. Paleoecological Studies in the Klokkeweel Bog near Hoogkarspel (Prov. of Noord-Holland). *Rev. Palaeobot. Palynol.* **1980**, *30*, 371–418. [CrossRef]
51. Van Geel, B. A Palaeoecological Study of Holocene Peat Bog Sections in Germany and The Netherlands, Based on the Analysis of Pollen, Spores and Macro- and Microscopic Remains of Fungi, Algae, Cormophytes and Animals. *Rev. Palaeobot. Palynol.* **1978**, *25*, 1–120. [CrossRef]
52. Van Geel, B. Non-Pollen Palynomorphs. In *Tracking Environmental Change Using Lake Sediments: Terrestrial, Algal, and Siliceous Indicators*; Smol, J.P., Birks, H.J.B., Last, W.M., Bradley, R.S., Alverson, K., Eds.; Developments in Paleoenvironmental Research; Springer: Dordrecht, The Netherlands, 2001; pp. 99–119. ISBN 978-0-306-47668-6.
53. Whitlock, C.; Larsen, C. Charcoal as a Fire Proxy. In *Tracking Environmental Change Using Lake Sediments: Terrestrial, Algal, and Siliceous Indicators*; Smol, J.P., Birks, H.J.B., Last, W.M., Bradley, R.S., Alverson, K., Eds.; Developments in Paleoenvironmental Research; Springer: Dordrecht, The Netherlands, 2001; pp. 75–97. ISBN 978-0-306-47668-6.
54. Stockmarr, J. Tablets with Spores Used in Absolute Pollen Analysis. *Pollen Spores* **1971**, *13*, 614–621.
55. Carrió, J.S.; Navarro, C.; Navarro, J.; Munuera, M. The Distribution of Cluster Pine (Pinuspinaster) in Spain as Derived from Palaeoecological Data: Relationships with Phytosociological Classification. *Holocene* **2000**, *10*, 243–252. [CrossRef]
56. López-Sáez, J.A.; López-Merino, L.; Alba-Sánchez, F.; Pérez-Díaz, S.; Abel-Schaad, D.; Carrión, J.S. Late Holocene Ecological History of Pinus Pinaster Forests in the Sierra de Gredos of Central Spain. *Plant Ecol.* **2009**, *206*, 195. [CrossRef]
57. López-Sáez, J.A.; Camarero, J.J.; Abel-Schaad, D.; Luelmo-Lautenschlaeger, R.; Pérez-Díaz, S.; Alba-Sánchez, F.; Carrión, J.S. Don't Lose Sight of the Forest for the Trees! Discerning Iberian Pine Communities by Means of Pollen-vegetation Relationships. *Rev. Palaeobot. Palynol.* **2020**, *281*, 104285. [CrossRef]
58. Schneider, R.R.; Price, B.; Müller, P.J.; Kroon, D.; Alexander, I. Monsoon Related Variations in Zaire (Congo) Sediment Load and Influence of Fluvial Silicate Supply on Marine Productivity in the East Equatorial Atlantic during the Last 200,000 Years. *Paleoceanography* **1997**, *12*, 463–481. [CrossRef]
59. Cornu, S.; Lucas, Y.; Lebon, E.; Ambrosi, J.P.; Luizão, F.; Rouiller, J.; Bonnay, M.; Neal, C. Evidence of Titanium Mobility in Soil Profiles, Manaus, Central Amazonia. *Geoderma* **1999**, *91*, 281–295. [CrossRef]
60. Thomson, J.; Croudace, I.W.; Rothwell, R.G. A Geochemical Application of the ITRAX Scanner to a Sediment Core Containing Eastern Mediterranean Sapropel Units. *Geol. Soc. Lond. Spec. Publ.* **2006**, *267*, 65–77. [CrossRef]
61. Burnett, A.P.; Soreghan, M.J.; Scholz, C.A.; Brown, E.T. Tropical East African Climate Change and Its Relation to Global Climate: A Record from Lake Tanganyika, Tropical East Africa, over the Past 90+kyr. *Palaeogeogr. Palaeoclimatol. Palaeoecol.* **2011**, *303*, 155–167. [CrossRef]
62. Chagué, C. Chapter 18—Applications of geochemical proxies in paleotsunami research. In *Geological Records of Tsunamis and Other Extreme Waves*; Engel, M., Pilarczyk, J., May, S.M., Brill, D., Garrett, E., Eds.; Elsevier: Amsterdam, The Netherlands, 2020; pp. 381–401. ISBN 978-0-12-815686-5.
63. Naeher, S.; Gilli, A.; North, R.P.; Hamann, Y.; Schubert, C.J. Tracing Bottom Water Oxygenation with Sedimentary Mn/Fe Ratios in Lake Zurich, Switzerland. *Chem. Geol.* **2013**, *352*, 125–133. [CrossRef]
64. Demina, L.L.; Novichkova, E.A.; Lisitzin, A.P.; Kozina, N.V. Geochemical Signatures of Paleoclimate Changes in the Sediment Cores from the Gloria and Snorri Drifts (Northwest Atlantic) over the Holocene-Mid Pleistocene. *Geosciences* **2019**, *9*, 432. [CrossRef]
65. Herrmann, S.; Stroncik, N. Data Report: Si, Al, Fe, Ca, and K Systematics of Volcaniclastic Sediments from Selected Cores of Hole U1347A, IODP Expedition 324. *Proc. IODP* **2013**, *324*. [CrossRef]
66. Hoelzmann, P.; Klein, T.; Kutz, F.; Schütt, B. A New Device to Mount Portable Energy-Dispersive X-Ray Fluorescence Spectrometers (p-ED-XRF) for Semi-Continuous Analyses of Split (Sediment) Cores and Solid Samples. *Geosci. Instrum. Methods Data Syst.* **2017**, *6*, 93–101. [CrossRef]
67. Santisteban, J.I.; Mediavilla, R.; de Frutos, L.G.; Cilla, I.L. Holocene Floods in a Complex Fluvial Wetland in Central Spain: Environmental Variability, Climate and Time. *Glob. Planet. Chang.* **2019**, *181*, 102986. [CrossRef]
68. Kaufman, D.S.; Ager, T.A.; Anderson, N.J.; Anderson, P.M.; Andrews, J.T.; Bartlein, P.J.; Brubaker, L.B.; Coats, L.L.; Cwynar, L.C.; Duvall, M.L.; et al. Holocene Thermal Maximum in the Western Arctic (0–180°W). *Quat. Sci. Rev.* **2004**, *23*, 529–560. [CrossRef]
69. Marcott, S.A.; Shakun, J.D.; Clark, P.U.; Mix, A.C. A Reconstruction of Regional and Global Temperature for the Past 11,300 Years. *Science* **2013**, *339*, 1198–1201. [CrossRef]
70. Liu, Z.; Zhu, J.; Rosenthal, Y.; Zhang, X.; Otto-Bliesner, B.L.; Timmermann, A.; Smith, R.S.; Lohmann, G.; Zheng, W.; Timm, O.E. The Holocene Temperature Conundrum. *Proc. Natl. Acad. Sci. USA* **2014**, *111*, E3501–E3505. [CrossRef]
71. Bova, S.; Rosenthal, Y.; Liu, Z.; Godad, S.P.; Yan, M. Seasonal Origin of the Thermal Maxima at the Holocene and the Last Interglacial. *Nature* **2021**, *589*, 548–553. [CrossRef]

72. Alley, R.B.; Ágústsdóttir, A.M. The 8k Event: Cause and Consequences of a Major Holocene Abrupt Climate Change. *Quat. Sci. Rev.* **2005**, *24*, 1123–1149. [CrossRef]
73. Rohling, E.J.; Pälike, H. Centennial-Scale Climate Cooling with a Sudden Cold Event around 8,200 Years Ago. *Nature* **2005**, *434*, 975–979. [CrossRef]
74. García-Artola, A.; Stéphan, P.; Cearreta, A.; Kopp, R.E.; Khan, N.S.; Horton, B.P. Holocene Sea-Level Database from the Atlantic Coast of Europe. *Quat. Sci. Rev.* **2018**, *196*, 177–192. [CrossRef]
75. Cacho, I.; Grimalt, J.O.; Canals, M.; Sbaffi, L.; Shackleton, N.J.; Schönfeld, J.; Zahn, R. Variability of the Western Mediterranean Sea Surface Temperature during the Last 25,000 Years and Its Connection with the Northern Hemisphere Climatic Changes. *Paleoceanography* **2001**, *16*, 40–52. [CrossRef]
76. Català, A.; Cacho, I.; Frigola, J.; Pena, L.D.; Lirer, F. Holocene Hydrography Evolution in the Alboran Sea: A Multi-Record and Multi-Proxy Comparison. *Clim. Past* **2019**, *15*, 927–942. [CrossRef]
77. Adkins, J.; de Menocal, P.; Eshel, G. The "African Humid Period" and the Record of Marine Upwelling from Excess 230Th in Ocean Drilling Program Hole 658C. *Paleoceanography* **2006**, *21*. [CrossRef]
78. Stumpf, R.; Frank, M.; Schönfeld, J.; Haley, B.A. Climatically Driven Changes in Sediment Supply on the SW Iberian Shelf since the Last Glacial Maximum. *Earth Planet. Sci. Lett.* **2011**, *312*, 80–90. [CrossRef]
79. Thornalley, D.J.R.; Elderfield, H.; McCave, I.N. Holocene Oscillations in Temperature and Salinity of the Surface Subpolar North Atlantic. *Nature* **2009**, *457*, 711–714. [CrossRef]
80. Bazzicalupo, P.; Maiorano, P.; Girone, A.; Marino, M.; Combourieu-Nebout, N.; Pelosi, N.; Salgueiro, E.; Incarbona, A. Holocene Climate Variability of the Western Mediterranean: Surface Water Dynamics Inferred from Calcareous Plankton Assemblages. *Holocene* **2020**, *30*, 691–708. [CrossRef]
81. Born, A.; Levermann, A. The 8.2 Ka Event: Abrupt Transition of the Subpolar Gyre toward a Modern North Atlantic Circulation. *Geochem. Geophys. Geosyst.* **2010**, *11*. [CrossRef]
82. Johnsen, S.J.; Clausen, H.B.; Dansgaard, W.; Gundestrup, N.S.; Hammer, C.U.; Andersen, U.; Andersen, K.K.; Hvidberg, C.S.; Dahl-Jensen, D.; Steffensen, J.P.; et al. The Δ18O Record along the Greenland Ice Core Project Deep Ice Core and the Problem of Possible Eemian Climatic Instability. *J. Geophys. Res. Oceans* **1997**, *102*, 26397–26410. [CrossRef]
83. Teixeira, S.B.; Gaspar, P.; Rosa, M. Holocene Sea-Level Index Points on the Quarteira Coast (Algarve, Portugal). In Proceedings of the Iberian Holocene Paleoenvironmental Evolution; University of Lisbon: Lisbon, Portugal, 2005; pp. 125–127.
84. Sousa, C.; Boski, T.; Pereira, L. Holocene Evolution of a Barrier Island System, Ria Formosa, South Portugal. *Holocene* **2019**, *29*, 64–76. [CrossRef]
85. Lambeck, K.; Rouby, H.; Purcell, A.; Sun, Y.; Sambridge, M. Sea Level and Global Ice Volumes from the Last Glacial Maximum to the Holocene. *Proc. Natl. Acad. Sci. USA* **2014**, *111*, 15296–15303. [CrossRef]
86. Trog, C.; Höfer, D.; Frenzel, P.; Camacho, S.; Schneider, H.; Mäusbacher, R. A Multi-Proxy Reconstruction and Comparison of Holocene Palaeoenvironmental Changes in the Alvor and Alcantarilha Estuaries (Southern Portugal). *Rev. Micropaleontol.* **2013**, *56*, 131–158. [CrossRef]
87. Delgado, J.; Boski, T.; Nieto, J.M.; Pereira, L.; Moura, D.; Gomes, A.; Sousa, C.; García-tenorio, R. Sea-Level Rise and Anthropogenic Activities Recorded in the Late Pleistocene / Holocene Sedimentary in Fi Ll of the Guadiana Estuary (SW Iberia). *Quat. Sci. Rev.* **2012**, *33*, 121–141. [CrossRef]
88. Schneider, H.; Höfer, D.; Trog, C.; Busch, S.; Schneider, M.; Baade, J.; Daut, G.; Mäusbacher, R. Holocene Estuary Development in the Algarve Region (Southern Portugal)—A Reconstruction of Sedimentological and Ecological Evolution. *Quat. Int.* **2010**, *221*, 141–158. [CrossRef]
89. Boski, T.; Camacho, S.; Moura, D.; Fletcher, W.; Wilamowski, A.; Veiga-Pires, C.; Correia, V.; Loureiro, C.; Santana, P. Chronology of the Sedimentary Processes during the Postglacial Sea Level Rise in Two Estuaries of the Algarve Coast, Southern Portugal. *Estuar. Coast. Shelf Sci.* **2008**, *77*, 230–244. [CrossRef]
90. Figueiral, I.; Carcaillet, C. A Review of Late Pleistocene and Holocene Biogeography of Highland Mediterranean Pines (Pinus Type Sylvestris) in Portugal, Based on Wood Charcoal. *Quat. Sci. Rev.* **2005**, *24*, 2466–2476. [CrossRef]
91. Fletcher, W.J.; Boski, T.; Moura, D. Palynological Evidence for Environmental and Climatic Change in the Lower Guadiana Valley, Portugal, during the Last 13 000 Years. *Holocene* **2007**, *4*, 481–494. [CrossRef]
92. Schröder, T.; van't Hoff, J.; López-Sáez, J.A.; Viehberg, F.; Melles, M.; Reicherter, K. Holocene Climatic and Environmental Evolution on the Southwestern Iberian Peninsula: A High-Resolution Multi-Proxy Study from Lake Medina (Cádiz, SW Spain). *Quat. Sci. Rev.* **2018**, *198*, 208–225. [CrossRef]
93. Morellón, M.; Aranbarri, J.; Moreno, A.; González-Sampériz, P.; Valero-Garcés, B.L. Early Holocene Humidity Patterns in the Iberian Peninsula Reconstructed from Lake, Pollen and Speleothem Records. *Quat. Sci. Rev.* **2018**, 1–18. [CrossRef]
94. Berger, A.L. Long-Term Variations of Caloric Insolation Resulting from the Earth's Orbital Elements. *Quat. Res.* **1978**, *9*, 139–167. [CrossRef]
95. Bond, G.; Showers, W.; Cheseby, M.; Lotti, R.; Almasi, P.; DeMenocal, P.; Priore, P.; Cullen, H.; Hajdas, I.; Bonani, G. A Pervasive Millennial-Scale Cycle in North Atlantic Holocene and Glacial Climates. *Science* **1997**, *278*, 1257–1266. [CrossRef]
96. Masson-Delmotte, V.; Jouzel, J.; Landais, A.; Stievenard, M.; Johnsen, S.J.; White, J.W.C.; Werner, M.; Sveinbjornsdottir, A.; Fuhrer, K. GRIP Deuterium Excess Reveals Rapid and Orbital-Scale Changes in Greenland Moisture Origin. *Science* **2005**, *309*, 118–121. [CrossRef]

97. Rasmussen, S.O.; Vinther, B.M.; Clausen, H.B.; Andersen, K.K. Early Holocene Climate Oscillations Recorded in Three Greenland Ice Cores. *Quat. Sci. Rev.* **2007**, *26*, 1907–1914. [CrossRef]
98. Pinto da Cruz, C.S.B. Temporary Ponds Vegetation and Dynamics: SW Portugal. Vegetação e Dinâmica dos Charcos Temporários do Sudoeste Alentejano. Ph.D. Thesis, University of Lisbon, Lisbon, Portugal, 1999.
99. López-Sáez, J.A.; Pérez-Díaz, S.; Rodríguez-Ramírez, A.; Blanco-González, A.; Villarías-Robles, J.J.R.; Luelmo-Lautenschlaeger, R.; Jiménez-Moreno, G.; Celestino-Pérez, S.; Cerrillo-Cuenca, E.; Pérez-Asensio, J.N.; et al. Mid-Late Holocene Environmental and Cultural Dynamics at the South-West Tip of Europe (Doñana National Park, SW Iberia, Spain). *J. Archaeol. Sci. Rep.* **2018**, *22*, 58–78. [CrossRef]
100. Fletcher, W.J. Holocene Landscape History of Southern Portugal. Ph.D. Thesis, University of Cambridge, Cambridge, UK, 2005.
101. Gomes, S.D.; Fletcher, W.J.; Rodrigues, T.; Stone, A.; Abrantes, F.; Naughton, F. Time-Transgressive Holocene Maximum of Temperate and Mediterranean Forest Development across the Iberian Peninsula Reflects Orbital Forcing. *Palaeogeogr. Palaeoclimatol. Palaeoecol.* **2020**, *550*, 109739. [CrossRef]
102. Oliveira, D.; Desprat, S.; Yin, Q.; Naughton, F.; Trigo, R.; Rodrigues, T.; Abrantes, F.; Goñi, M.F.S. Unraveling the Forcings Controlling the Vegetation and Climate of the Best Orbital Analogues for the Present Interglacial in SW Europe. *Clim. Dyn.* **2018**, *51*, 667–686. [CrossRef]
103. Chabaud, L.; Goñi, M.F.S.; Desprat, S.; Rossignol, L. Land–Sea Climatic Variability in the Eastern North Atlantic Subtropical Region over the Last 14,200 Years: Atmospheric and Oceanic Processes at Different Timescales. *Holocene* **2014**, *24*, 787–797. [CrossRef]
104. Renssen, H.; Goosse, H.; Fichefet, T.; Campin, J.-M. The 8.2 Kyr BP Event Simulated by a Global Atmosphere—Sea-Ice—Ocean Model. *Geophys. Res. Lett.* **2001**, *28*, 1567–1570. [CrossRef]
105. Reed, J.M.; Stevenson, A.C.; Juggins, S. A Multi-Proxy Record of Holocene Climatic Change in Southwestern Spain: The Laguna de Medina, Cádiz. *Holocene* **2001**, *11*, 707–719. [CrossRef]
106. Nebout, N.C.; Peyron, O.; Dormoy, I.; Desprat, S.; Beaudouin, C.; Kotthoff, U.; Marret, F. Rapid Climatic Variability in the West Mediterranean during the Last 25 000 Years from High Resolution Pollen Data. *Clim. Past* **2009**, *5*, 503–521. [CrossRef]
107. Fletcher, W.J.; Goñi, M.F.S. Orbital- and Sub-Orbital-Scale Climate Impacts on Vegetation of the Western Mediterranean Basin over the Last 48,000 Yr. *Quat. Res.* **2008**, *70*, 451–464. [CrossRef]
108. Schröder, T.; López-Sáez, J.A.; van't Hoff, J.; Reicherter, K. Unravelling the Holocene Environmental History of South-Western Iberia through a Palynological Study of Lake Medina Sediments. *Holocene* **2019**, *30*, 13–22. [CrossRef]
109. Manzano, S.; Carrión, J.S.; López-Merino, L.; Ochando, J.; Munuera, M.; Fernández, S.; González-Sampériz, P. Early to Mid-Holocene Spatiotemporal Vegetation Changes and Tsunami Impact in a Paradigmatic Coastal Transitional System (Doñana National Park, Southwestern Europe). *Glob. Planet. Chang.* **2018**, *161*, 66–81. [CrossRef]
110. Cortés-Sánchez, M.; Jiménez-Espejo, F.J.; Simón-Vallejo, M.D.; Gibaja-Bao, J.F.; Faustino Carvalho, A.; Martínez-Ruiz, F.; Rodrigo Gamiz, M.; Flores, J.-A.; Paytan, A.; López-Sáez, J.A.; et al. The Mesolithic—Neolithic Transition in Southern Iberia. *Quat. Res.* **2012**, *77*, 221–234. [CrossRef]
111. Costas, S.; Ferreira, Ó.; Plomaritis, T.A.; Leorri, E. Coastal Barrier Stratigraphy for Holocene High-Resolution Sea-Level Reconstruction. *Sci. Rep.* **2016**, *6*, 38726. [CrossRef]
112. Lario, J.; Luque, L.; Zazo, C.; Goy, J.L.; Spencer, C.; Cabero, A.; Bardají, T.; Borja, F.; Dabrio, C.J.; Civis, J.; et al. Tsunami vs. Storm Surge Deposits: A Review of the Sedimentological and Geomorphological Records of Extreme Wave Events (EWE) during the Holocene in the Gulf of Cadiz, Spain. *Z. Geomorphol. Suppl. Issues* **2010**, *54*, 301–316. [CrossRef]
113. Dias, J.M.A.; Boski, T.; Rodrigues, A.; Magalhães, F. Coast Line Evolution in Portugal since the Last Glacial Maximum until Present—A Synthesis. *Mar. Geol.* **2000**, *170*, 177–186. [CrossRef]
114. McLaughlin, T.R.; Gómez-Puche, M.; Cascalheira, J.; Bicho, N.; Fernández-López de Pablo, J. Late Glacial and Early Holocene Human Demographic Responses to Climatic and Environmental Change in Atlantic Iberia. *Philos. Trans. R. Soc. B Biol. Sci.* **2020**, *376*, 20190724. [CrossRef]
115. Bicho, N.F. The End of the Paleolithic and the Mesolithic in Portugal. *Curr. Anthropol.* **1994**, *35*, 664–674. [CrossRef]
116. Bicho, N.; Umbelino, C.; Detry, C.; Pereira, T. The Emergence of Muge Mesolithic Shell Middens in Central Portugal and the 8200 Cal Yr BP Cold Event. *J. Isl. Coast. Archaeol.* **2010**, *5*, 86–104. [CrossRef]
117. Pereira, T.; Carvalho, A.F. Abrupt Technological Change at the 8.2 Ky Cal BP Climatic Event in Central Portugal. The Epipalaeolithic of Pena d'Água Rock-Shelter. *Comptes Rendus Palevol* **2015**, *14*, 423–435. [CrossRef]
118. Pereira, T.; Andrade, C.; Costa, M.; Farias, A.; Mirão, J.; Carvalho, A.F. Lithic Economy and Territory of Epipaleolithic Hunter–Gatherers in the Middle Tagus: The Case of Pena d'Água (Portugal). *Quat. Int.* **2016**, *412*, 135–144. [CrossRef]
119. Stjerna, R.P. *On Death in the Mesolithic: Or the Mortuary Practices of the Last Hunter-Gatherers of the South-Western Iberian Peninsula, 7th–6th Millennium BCE*; Department of Archaeology and Ancient History, Uppsala University: Uppsala, Sweden, 2016.
120. Bicho, N.; Cascalheira, J.; Gonçalves, C.; Umbelino, C.; Rivero, D.G.; André, L. Resilience, Replacement and Acculturation in the Mesolithic/Neolithic Transition: The Case of Muge, Central Portugal. *Quat. Int.* **2017**, *446*, 31–42. [CrossRef]
121. Valente, M.J. Mesolithic and Neolithic Shell Middens in Western Algarve: Issues in Ecology, Taphonomy and Economy. In *Proceedings of the First Zooarchaeology Conference in Portugal, University of Lisbon, Lisbon, Portugal, 2012*; Detry, C., Dias, R., Eds.; University of Lisbon: Lisbon, Portugal, 2012; pp. 24–32.

122. Brisset, E.; Burjachs, F.; Ballesteros Navarro, B.J.; Fernández-López de Pablo, J. Socio-Ecological Adaptation to Early-Holocene Sea-Level Rise in the Western Mediterranean. *Glob. Planet. Chang.* **2018**, *169*, 156–167. [CrossRef]
123. Carvalho, A.F.; Petchey, F. Stable Isotope Evidence of Neolithic Palaeodiets in the Coastal Regions of Southern Portugal. *J. Isl. Coast. Archaeol.* **2013**, *8*, 361–383. [CrossRef]
124. López-Sáez, J.A.; Pérez-Díaz, S.; Alba, F. Antropización y Agricultura En El Neolítico de Andalucía Occidental a Partir de La Palinología. *Menga* **2011**, *2*, 72–85.
125. Lario, J.; Zazo, C.; Goy, J.L.; Silva, P.G.; Bardaji, T.; Cabero, A.; Dabrio, C.J. Holocene Palaeotsunami Catalogue of SW Iberia. *Quat. Int.* **2011**, *242*, 196–200. [CrossRef]